PRODUCTION AND ANALYSIS OF LITHIUM ION BEAMS IN THE LOW ELECTRON VOLT REGION

WALKER W. LAMBERT

PRODUCTION AND ANALYSIS OF LITHIUM ION BEAMS IN THE LOW ELECTRON VOLT REGION

* * * * * *

Walker W. Lambert

PRODUCTION AND ANALYSIS OF LITHIUM ION BEAMS IN THE LOW ELECTRON VOLT REGION

by

Walker W. Lambert
//
Lieutenant, United States Navy

Submitted in partial fulfillment of
the requirements for the degree of

MASTER OF SCIENCE
IN
PHYSICS

United States Naval Postgraduate School
Monterey, California

1 9 6 3

NPS Archives
1963
Lambert, W.

PRODUCTION AND ANALYSIS OF LITHIUM ION BEAMS IN THE LOW ELECTRON VOLT REGION

by

Walker W. Lambert

This work is accepted as fulfilling
the thesis requirements for the degree of
MASTER OF SCIENCE
IN
PHYSICS
from the
United States Naval Postgraduate School

ABSTRACT

A lithium ion source capable of delivering low energy, monoenergetic beams of rectangular cross section, has been developed for use in the study of low-energy atomic, ionic, and molecular impact phenomena. An analysis of the spatial and energy distribution of the ion beams extracted from the source was made over the range of ion energies from 1.2 ev. to 100 ev. with particular attention given to beams with energies less than 25 ev. The experimental equipment and procedures are described. For the beams of low energy the intensity of the beam was limited by the space charge. The beam intensity in this space charge limited condition was approximately one third of the theoretical limit. Total beam intensities ranged from a few times 10^{-8} amps at the lowest energies to a few times 10^{-7} amps at the higher energies with corresponding energy spreads of $\pm$.1 eV to $\pm$ 0.3 eV. Typical beam dimensions are 1.0 cm by 2.0 cm at a distance of 5.0 cm from the gun with an aperture 0.47 cm by 1.5 cm.

The writer wishes to express his appreciation for the assistance and encouragement given him by Professor Otto Heinz of the U. S. Naval Postgraduate School and for the experimental and technical assistance given him by Dr. D.C. Lorents and Mr. R. Leon of Stanford Research Institute in the course of this investigation.

TABLE OF CONTENTS

LIST OF ILLUSTRATIONS

Table of Symbols and Abbreviations

d - distance between electrodes

e - charge of the electron

$\bar{E}$ - average energy of the ion beam

ΔE - energy spread

I_c - collector current

I_i - ion current

J_i - ion current density

k - the Boltzmann constant

m_i - mass of ion

M_i - atomic weight of ion

n - ionization state of Ions

T - temperature of the emitter

V_a - accelerating potential

V_d - stopping potential applied to slit plate

x - distance along beam axis

ϵ - base of Naperian logarithms

φ - work function

I. INTRODUCTION

A lithium (or other alkali) ion source capable of delivering low energy, monoenergetic beams has been developed for use in the study of low-energy atomic, ionic, and molecular impact phenomena. The energies of interest in this research are in the 0.5 to 25 ev. range for both the ion beams and the neutral beams obtainable from them. These energies are considerably above the energies of "thermal" beams (.02-.2 ev.) and below the energies easily produced by the more conventional ion sources employing some form of gaseous plasma. Since theoretical treatments of interactions in this energy range are difficult, we must at present rely largely on experimental data for our understanding of these processes. On the other hand one of the difficulties in developing a detailed theory in this energy range is the scarcity of experimental data on such low-energy reactions as charge-transfer, ionization by electronic collisions, elastic and inelastic scattering processes, ion-atom interchange, surface reactions, etc.

In the past, experimental techniques for studying reactions of neutral particles in this energy range in the laboratory have been limited to the shock tube. While many important results were obtained from this work, the development of more direct methods of measurement of cross sections and reaction rates would be extremely valuable.

At the present time, there seem to be two schemes for producing beams of atoms or molecules in the desired range. A method developed at Cornell Aeronautical Laboratory[1] obtains a beam from a shocked gas. The Kantrowitz-Grey[2] expansion nozzle is used to expand the shocked gas, reducing its temperature and increasing the translational velocity of the gas.

The second method begins with a reasonably mono-energetic ion beam and partially transforms this ion beam to a neutral beam by a charge-transfer of the type $A^+ + B \rightarrow A + B^+$. This method has previously been used to produce neutral beams at energies down to 25 ev.[3] At energies below 25 ev. the attainable beam intensities are low due to space charge limits on the intensity of the ion beam, but with refined detection techniques this is not too serious a limitation.

The alkali ion source reported here is able to provide well defined ion beams (both spatially and in energy) of useable intensity. By the use of the charge-transfer process in a gas corresponding neutral beams of comparable intensity, energy and spatial distribution should be obtainable from this ion beam. We thus have a primary beam which can be used either directly (ions) or after charge-transfer (neutrals). By directing this primary beam into a gas or permitting it to interact with another molecular beam, reactions of known species can be observed and their interaction cross-sections measured as a function of energy.

II. EXPERIMENTAL EQUIPMENT AND PROCEDURES

The experimental equipment for carrying out this research project consists of:

1. The vacuum system
2. The experimental chamber
3. The ion gun
4. The ion collectors
5. Measuring instruments

The vacuum system is a high volume, high vacuum pumping station upon which is mounted the experimental chamber. A detailed description of the vacuum system and the experimental chamber is found in Appendix 1. The vacuum system is capable of providing working pressures of 1.0×10^{-7} torr to 1.0×10^{-6} torr in the experimental chamber.

The ion gun consists of an emitter and accelerating electrodes which are mounted in a lavite holder to provide maximum freedom to adjust the parameters of the ion gun. The principal features of the ion gun are shown in Fig. 1. The design of the electrodes is based on the Pierce principle of focusing space charge limited beams of charged particles [4].

The lithium ions are produced by thermionic emission from the mineral beta-eucryptite on the face of tantalum emitter. The emitter is heated by a tungsten filament which is wound in a flat coil and embedded in Alundum cement inside the emitter boat. The mineral

Figure 1

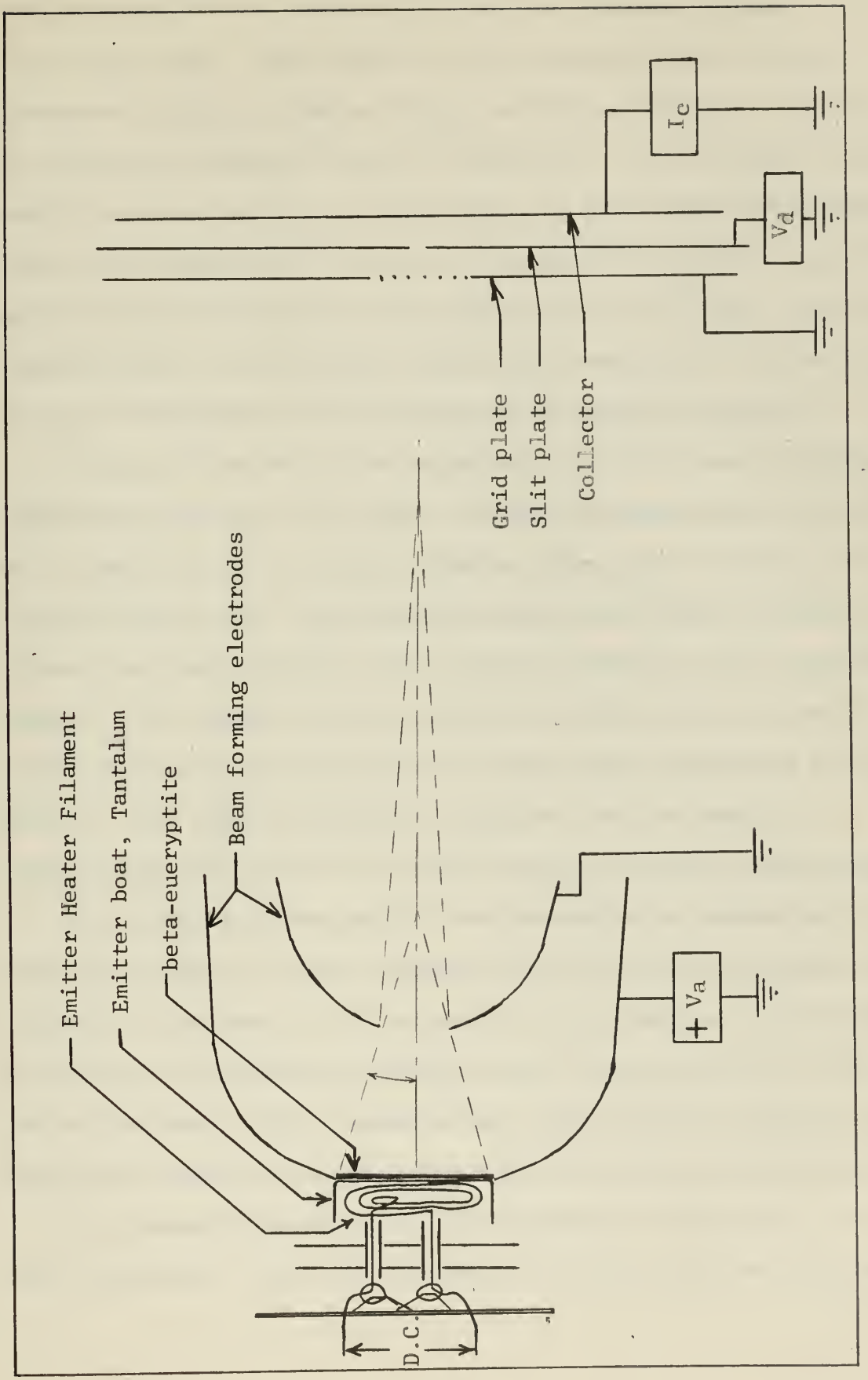

Figure 1. Schematic of ion gun and the collector used for analyzing the energy of the beam (side views).

beta-eucryptite is a ceramic that has the chemical formula $Li_2O\ Al_2O_3\ 2SiO_2$. This material may be produced from Lithium Carbonate (Li_2CO_3), Alumina (Al_2O_3) and Silica (SiO_2) as described by Allison and Kamegai[5] and by Waldron.[6] The Li^+ beam from this source has been found to be quite pure. A crude mass spectrograph search for impurities by Allison and Kamegai[5] revealed a peak at mass 23 with an intensity of 5% relative to the Li^7 peak. This was presumably Na^+ but could have conceivably been LiO^+. Further details of the construction of the ion gun may be found in Appendix 2.

During the course of the experiment three ion beam collector assemblies were used. The first collector assembly used consisted of a simple 2.0 by 2.25 inch stainless steel paddle mounted on a stainless steel rod. The assembly entered the chamber through a Wilson type seal mounted on the side-port-flange of the experimental chamber. The purpose of this collector assembly was to measure the total ion beam and to determine the approximate horizontal beam profile. The total ion beam was measured over the range of accelerating potentials for several values of emitter temperature.

The horizontal beam profile was determined by measuring the total ion current to the collector as the collector was moved across the path of the beam. The increase in total beam was then determined for each mm. of collector movement until the collector was intercepting the entire beam. This procedure was used to give an approximate horizontal profile, and was not intended to be an exact determination.

The second collector assembly consisted of two parts, a slit plate and a collector. The slit plate was a 2.25 by 2.25 inch stainless

steel plate with a one-sixteenth inch horizontal slit running the width of the plate. The collector was a plain two by two inch stainless steel plate which was mounted one-fourth inch behind the slit plate on ceramic standoffs. The collector was mounted on a stainless steel rod which entered the top of the chamber through a Wilson seal and was free to move vertically. The purpose of this collector was to determine vertical profiles of the beam at all energies and for several values of emitter temperature. The vertical profile was determined by measuring the ion current that passed through the slit as the collector assembly was moved vertically through the beam. The slit plate was at ground potential and the collector plate was grounded through the micro-microammeter.

The third collector assembly was similar to the second collector assembly except that there was a grid located in front of the slit. A schematic of this collector is shown in Fig. 1. The main purpose of this collector assembly was to obtain an energy analysis of the beam. The grid plate consisted of a two by two inch stainless steel plate with a 0.25 inch slit horizontally across the center. A grid was constructed of 0.005 inch diameter nickel wire spaced 20 vertical wires per inch and two horizontal wires running the length of the 0.25 inch slit. The grid had approximately 90% open area for minimum beam attenuation. For further beam profile determination using this collector assembly, both the grid plate and slit plate were at ground potential and the ion current reaching the collector through the one mm. slit was measured on the micro-microammeter as the collector assembly was moved vertically through the beam. For energy analysis of the ion beam the grid plate was

at ground potential, but the slit plate was connected to the high voltage power supply. A positive decelerating potential is applied to the slit plate. The decelerating potential creates an electric field between the slit plate and the grid. The electric field opposes the direction of the flow of ions in the ion beam. When this decelerating potential is equal to the energy of the ion beam, the beam will be stopped at the slit plate and will not be measured by the micro-microammeter. The ion current reaching the collector was measured as the decelerating potential was increased from zero to a value greater than the value of the accelerating potential of the ion gun.

A Keithley 410 micro-microammeter was used for all collector current readings. This micro-microammeter is stepped in 20 scales with the full scale readings going from 10×10^{-4} amps, 3×10^{-5} amps, etc. to 3×10^{-13}. The accuracy of this meter is stated to be better than 2% in the range from 10×10^{-4} amps through 3×10^{-7} amps and better than 4% in the ranges from 10×10^{-9} through 3×10^{-13} amps. The micro-microammeter was checked in the laboratory and was found to have accuracies at least twice as good as those stated by the manufacturer. The micro-microammeter has a constant +216 volt outlet which is used as the source of the accelerating potential for the ion gun. The actual accelerating voltage is controlled by a potential divider and is variable from zero to 200 volts. The decelerating potential is supplied with a Keithley 240 high voltage power supply. The power supply is stepped in one volt steps from zero to 99 volts with an additional fine control to give fractional voltages.

The temperature of the emitter was measured by the use of a Leeds and Northrup optical Pyrometer. The face of the emitter is viewed through a Lucite port mounted on the front flange of the experimental chamber. The face of the emitter is clearly visible through this port when the collector is pulled out of the line of the ion beam.

An attempt was made to determine the composition of the emitted ion beam by a time of flight technique employing short (0.1 μsec.) pulses on the accelerating and collecting apertures. Due to the geometry and wiring of the present gun and collector we were unable to get sufficiently short rise times to carry this measurement out. It is believed, however, that with certain modifications in the pulse circuiting, this technique will yield a fair idea of the beam constitutents.

III. THEORETICAL CONSIDERATIONS

The emission of charged particles from a heated surface is known as thermionic emission. The thermionic emission of electrons from a heated surface is known to follow Richardson's Law which is

$$J = A T^2 \epsilon^{-\frac{e\varphi}{kT}}$$

where

J = current density from the emitter

A = a constant

T = temperature of the emitting surface, (^{o}K)

e = the charge of the electron

φ = the work function of the emitting surface

ϵ = the base of Naperian logarithms

k = the Boltzmann constant

The thermionic emission of ions of the alkali metals follows the form of Richardson's Law with a change in the number assigned to the constant A and the value of the constant φ (corresponding to the work function in the case of electron emission). This value is dependent on the composition of the material containing the alkali atoms, the accelerating field that is present at the emitting surface, and the ionization potential of the alkali metal in question. To demonstrate this correspondence a measurement was made of the total ion beam current as the temperature of the emitter was increased from 600^{o}C to 825^{o}C. The accelerating potential was held constant at ten volts. A plot of these measurements is shown in Figure 2, plotted as

$$ln \frac{I}{T^2} \quad \text{versus} \quad \frac{1}{T}$$

Figure 2

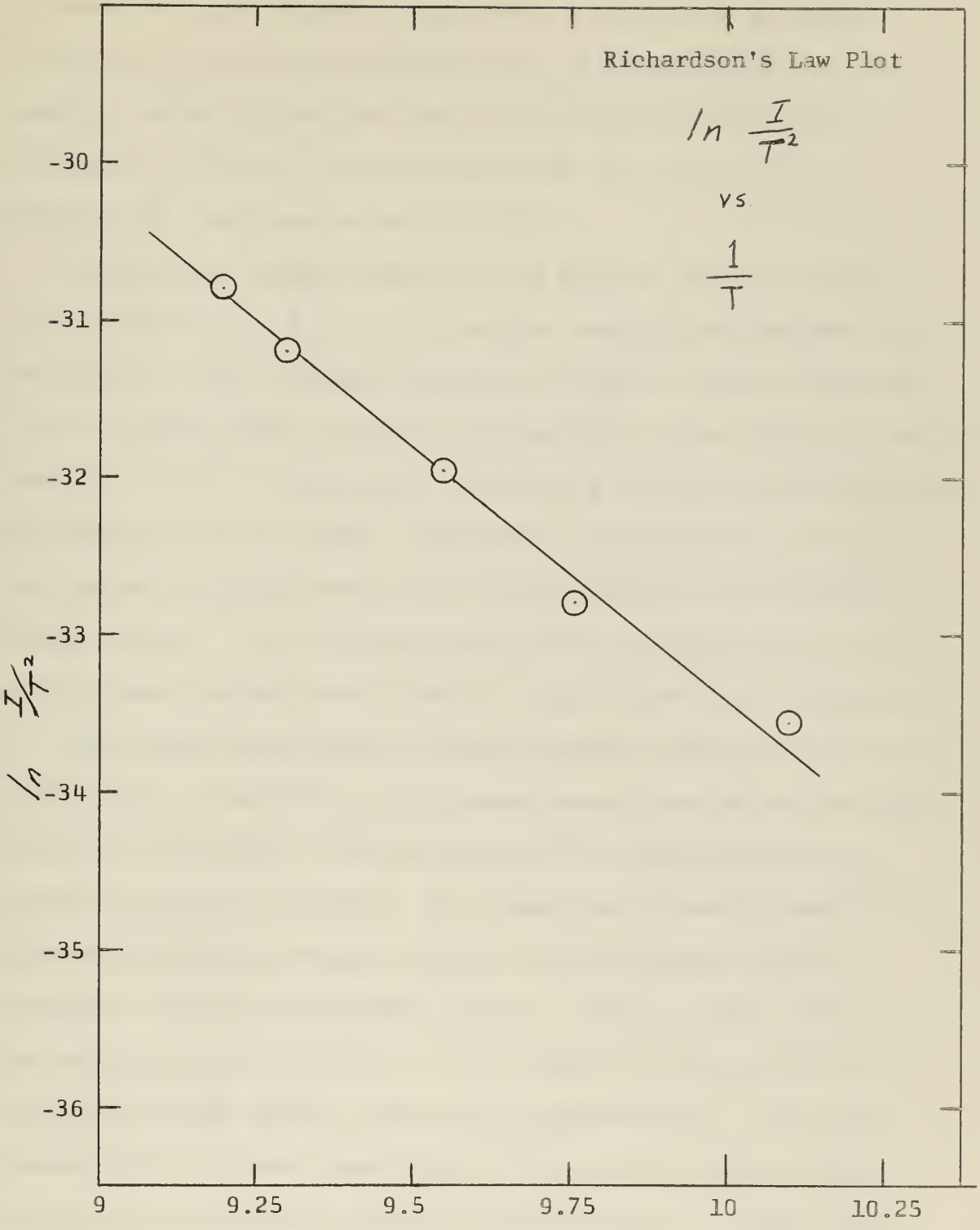

Figure 2. Richardson's Law Plot, $\ln \frac{I}{T^2}$ vs $\frac{1}{T}$

to check the application of Richardson's Law to the thermionic emission of ions from a substance such as beta-eucryptite. The measured values follow the form of the equation very closely. The slope of the plot was determined and the value of the constant φ, was found to be 2.9 volts.

The average thermal energy of the emitted ions is on the order of 0.08 ev to 0.11 ev for emitter temperatures between 650°C and 1000°C. These thermal energies are much less than the energy of the ion beam after acceleration, however, in the region of energies less than five ev, the thermal energy is a noticeable percentage of the energy of the ion beam. Therefore, at the very low energies the thermal energies constitute a major portion of the observed energy spread. It is therefore advisable to operate the ion gun at the lowest temperature at which a usable beam can be obtained.

The space charge effect in high intensity beams is due to the large number of particles of the same charge exerting coulomb type forces on one another. As the energy of a horizontal beam of charged particles is reduced, the transverse spreading produced by space charge forces becomes greater since the charge density increases with decreasing beam energy. Figure 3 shows plots of the heights of one and five ev. Li^+ beams, at five and ten cm. from the starting point, versus the current density. This plot assumes that the beam starts from a long, 1.0 cm. high aperture with all ions traveling parallel to the beam axis. This figure

Figure 3

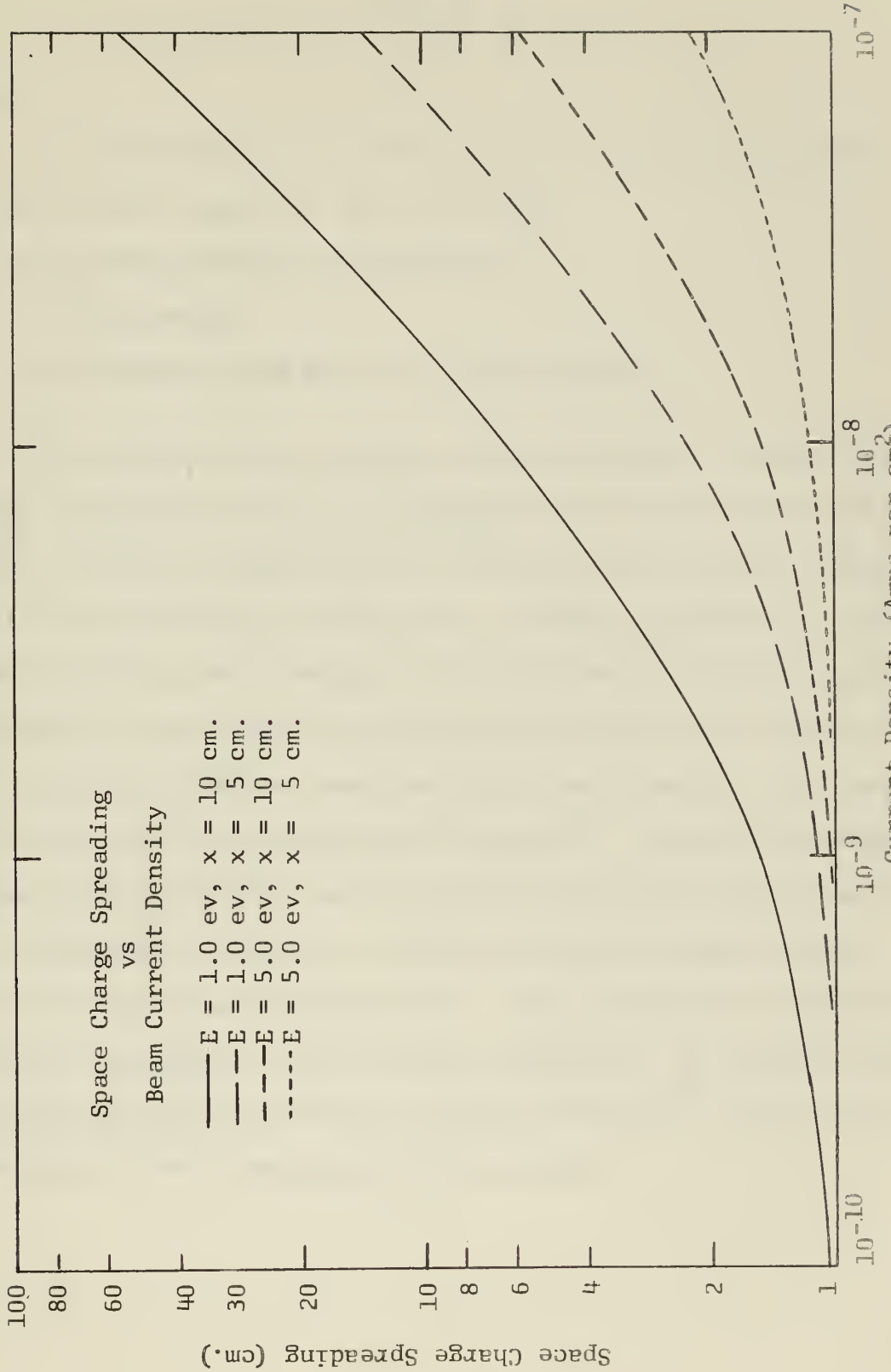

Figure 3. Space charge spreading of Li^+ beam

was drawn from the equation given by Von Ardenne[7]

$$y = 1.02 \times 10^{6} \frac{\sqrt{M_i J_i}}{V^{3/2}} x^2 + 1$$

where

y = semi-height of beam measured from the axis of the beam

M_i = atomic weight of ion (7 for Li^+)

J_i = current density at aperature

V = beam energy

X = distance along beam axis from aperature

As may be seen from the plot, the spreading of the very low energy horizontal beams is considerable as one moves away from the source. Since the beam energy is very low, space charge compensation due to free electrons is neglected. In order to decrease the space charge spreading one attempts to focus the beam in such a manner as to produce a beam which is converging as it leaves the emitter. The Pierce principle has been used quite extensively in the design of electron guns for high intensity beams.[8] Briefly, according to the Pierce principle, one design the electrodes of the beam so as to establish a potential function at the beam edge identical with that due to space limited flow. From experimental considerations, a beam of rectangular cross-section is desired. An electrode geometry utilizing the Pierce principle has been developed[7] which gives converging beams of rectangular cross-section.

The intensity of any beam is limited by the effect of the space charge in the vicinity of the emitter. The space charge limited ion current density for parallel electrodes is given by[7]

$$J_{io} = \frac{1}{9\pi} \frac{V_a^{3/2}}{d^2} \sqrt{\frac{2ne}{m_i}} = 5.45 \times 10^{-7} \frac{V_a^{3/2}}{d^2} \sqrt{\frac{n}{M_i}}$$

where

J_{io} = ion current density, amps / cm^2

n = ionization number

e = elementary charge

m_i = mass of ion

V_a = accelerating potential

d = distance between electrodes

M_i = atomic weight of ion

The current density for geometries other than parallel electrodes may be found by multiplying by a factor, C, which depends on the geometry adopted, the spacing of the electrodes, and the relative size of the aperature and emitter. The value of C for the geometry which was adopted for this experiment is 0.55. The current density is then

$$J_i = 0.55\, J_{io}$$

Using the appropriate values in the above equations we will have a maximum beam current of

$$I = 1.7 \times 10^{-8}\, V_a^{3/2}$$

for the 1.5 cm^2 emitter employed in this experiment.

IV. RESULTS

The early stages of the experiment were devoted to the construction of the Lithium ion source. During this phase the principal interest was in the total ion beam emitted from the gun. This total beam was studied as functions of emitter temperature and acceleration potential. Figures 4 and 5 show plots of total beam current versus accelerating potential as functions of the temperature of the emitter. When there was no accelerating potential on the electrodes, there was a small negative current to the collector due to the thermal electrons from the emitter. As a small accelerating potential is applied the ion beam begins to form. The accelerating potential at which the beam becomes positive varies with the emitter temperature and the configuration of the emitter. The range of this cross over point was from 0.25 volt to 2 volts. As the accelerating potential is increased the current increases in proportion to the space charge limit current. Fig. 6 shows the plot of total beam current versus the accelerating potential on a log-log plot. The space charge limited emitted current was computed and is shown for the geometry of our gun. The theoretical space charge current was not reached, the current which reaches the collector was approximately one-third of the space charge limited current for the low range of acceleration potentials. The upper limit of the range of proportionality varies with the temperature of the emitter. At higher accelerating potentials the ion current leveled off and became essentially constant. The

level off current was a function of emitter temperature.

From this analysis it was determined that due to the space charge limit effect it would not be profitable to increase emitter temperature beyond 850°C for the study of ions of energies less than 25ev. A measurement of the horizontal profile of the ion beam was made to determine the lateral spreading of the beam. Since the ion gun was not constructed to give any intensification in this dimension, it was expected that the horizontal width of the beam would be greater than 1.5 cm width of the opening in the electrodes of the gun. Figure 7 shows the plot of ion current per millimeter width versus the horizontal position of the collector at five, ten, and fifteen volts of accelerating potential. The widths of the beam as measured at one half of maximum beam were 2.7 cm, 2.0 cm and 1.9 cm at accelerating potentials of five, ten, and fifteen volts respectively. The collector was 6.7 cm from the face of the emitter for these measurements. These measurements were intended to give a rough indication of the beam width to be used in design of the collector for determining the vertical profile. It appeared that a two inch wide collector would be able to collect essentially all the beam in the horizontal dimension.

The second collector was used to obtain the height or thickness of the rectangular shaped beam. The horizontal slit passed a small slice of the ion beam over the full width of the beam. The collector was moved vertically and the beam was probed to obtain vertical profiles of the beam at several values of accelerating potential, emitter temperature, and distance of the collector from the emitter. Figures 8 through 14 show these vertical profiles as plots of collector

current per mm. versus the vertical position of the collector. The height of the ion beam was measured at one half of maximum ion intensity. While obtaining these vertical profiles, it was found that at a point well above the path of the main beam, there was a secondary beam, therefore, it appeared that this secondary beam was coming from the edges of the emitter behind the first accelerating electrode where the emitter joined the electrode.

Figure 15 shows a summary of the beam heights plotted against acceleration potential for the various emitter temperatures and distances from emitter. As expected, the beam height decreases with accelerating potential. The beam height is shown to increase with the temperature of the emitter. The random velocity due to thermal emission is not of sufficient magnitude to cause an effect this large, but the increase in temperature increases the total beam (below space charge limit) hence the ion density increases, causing greater space charge divergence. The space charge divergence at increased distances from the emitter is definitely observable. The predicted convergence of the beam at positions closer to the emitter is not evident as the smallest beam height is equal to the height of the opening in the front accelerating electrode.

The third collector unit was used to obtain an energy analysis of the ion beam. A positive potential applied to the slit plate sets up an electric field between the slit plate and the grid which acted as a stopping potential. When an ion beam with energy greater than the stopping potential approaches the collector it may be slowed but should pass through the slit without attenuation of beam

current. When the ion beam is of equal energy to the stopping potential, essentially all the beam should be stopped at the slit plate. Assuming that the spread in energies is isotropic the potential at one-half the initial ion current should be equal to the initial energy of the ion beam. When stopping or decelerating potential is greater than the ion beam energy, there should be no ion current reaching the collector.

Figures 15 through 18 show plots of ion current versus decelerating potential for several values of accelerating potential. Table I lists the average beam energies and energy spread of the beam for the different values of accelerating potential and emitter temperature. The beam energy was determined by the decelerating potential at one-half initial ion current. The energy spread (ΔE) was determined by the difference in potential between the values of decelerating potentials at both 90% and 10% of initial ion current, and at 75% and 25% of initial ion current.

TABLE I.

Average Beam Energies and Energy Spread

V_a(volts)	T (^oC)	$\overline{E}$(ev.)	ΔE(ev.) (.25-.75)	ΔE(ev.) (.10-.90)
1.6	795	1.2	0.7	1.2
2.0	820	1.3	0.3	0.5
2.0	795	1.5	0.3	0.9
3.0	790	1.9	0.3	0.5
3.0	800	2.4	0.2	0.4
5	800	3.95	0.4	0.6
10	800	8.4	0.5	1.0
15	805	13.4	0.6	1.3
15	805	13.9	1.1	1.9
25	810	24.1	1.8	3.2
50	810	49	3.0	6
100	810	101	5.5	11

The increase in ion current just before the value of the beam energy is reached is believed to be due to a focusing effect due to non-parallel field lines in the stopping field. This effect was not observed in two instances at very low energies and at present there is no apparent reason to explain this anomaly.

While obtaining the data for the analysis of the energy, in some instances the ion current, after reaching near zero at decelerating potentials equal to or slightly greater than the accelerating potential on the ion gun, would begin to increase linearly with an increase in decelerating potential. This effect

was found to be an ohmic current through the collector assembly. The collector assembly employed lucite washers for insulation between the collector and the grid and slit plates and the assembly was held together with nylon screws. When either the lucite washers or the nylon screws reach sufficiently high temperatures through radiation heating from the emitter of the ion gun, they begin to conduct. This effect occured only at the high emitter temperatures. The resistance of the washers or screws was determined to be approximately 10^{+9} to 10^{+10} ohms. The collector assembly was replaced by one using ceramic washers and ceramic screws.

V. SUMMARY

It has been demonstrated that low energy alkali ion beams of usable intensity and narrow energy dispersion can be produced from a thermal emitter and shaped by proper arrangement of the accelerating electrodes. It is known that under proper conditions, a reasonable fraction (up to one-third) of the ion beam may be converted into a neutral beam by the process of (resonant) charge exchange. We thus have a versatile tool for the investigation of low energy atomic collision processes.

While this particular emission technique can only be applied to a limited number of ions, namely the alkalis, many of the problems encountered here are common to all low energy ion beams. Particularly the question of beam formation and the problem of space charge spreading of the beam will be encountered in other sources as well.

Figure 4

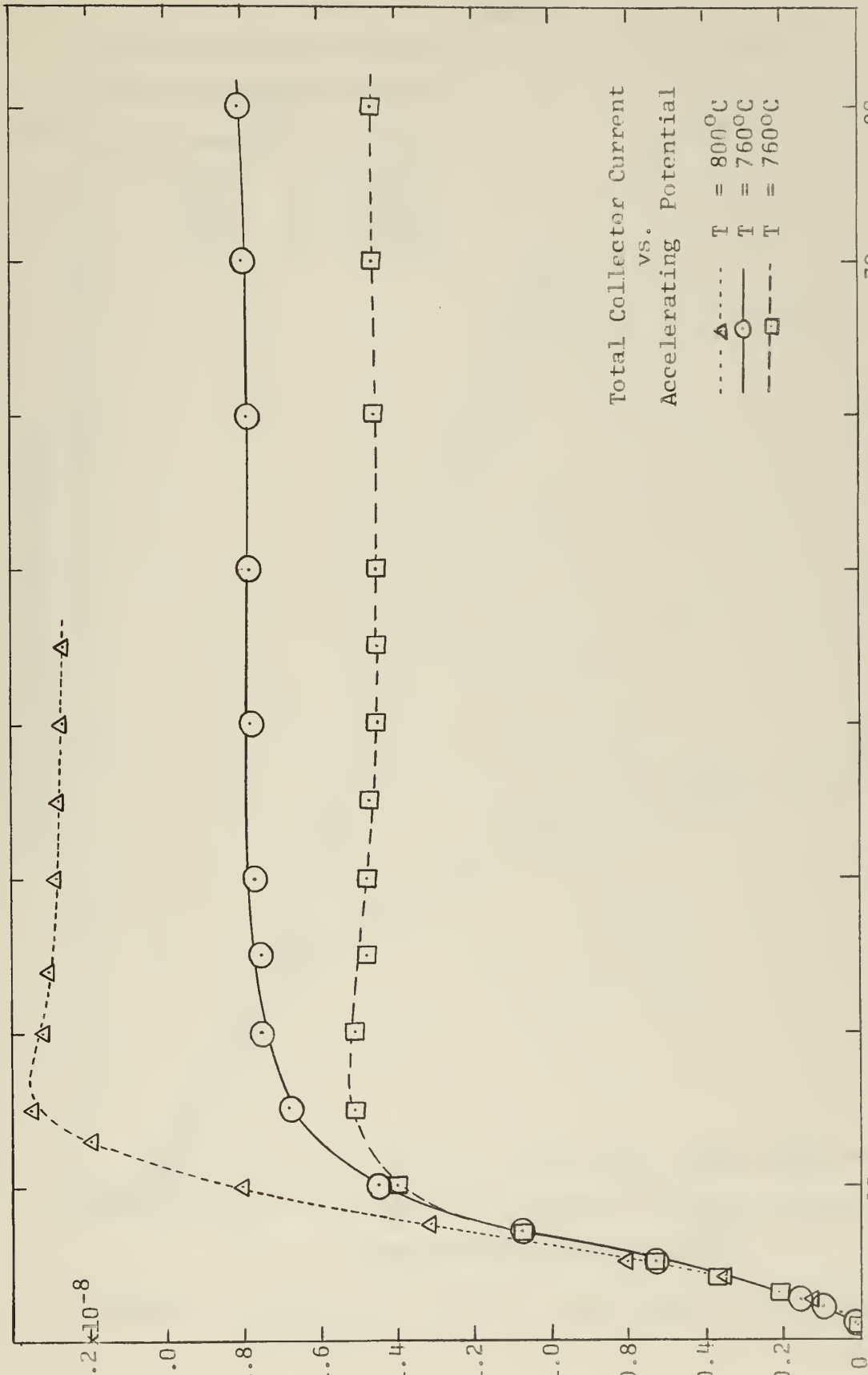

Figure 4. Total beam current as a function of accelerating potential.

Figure 5

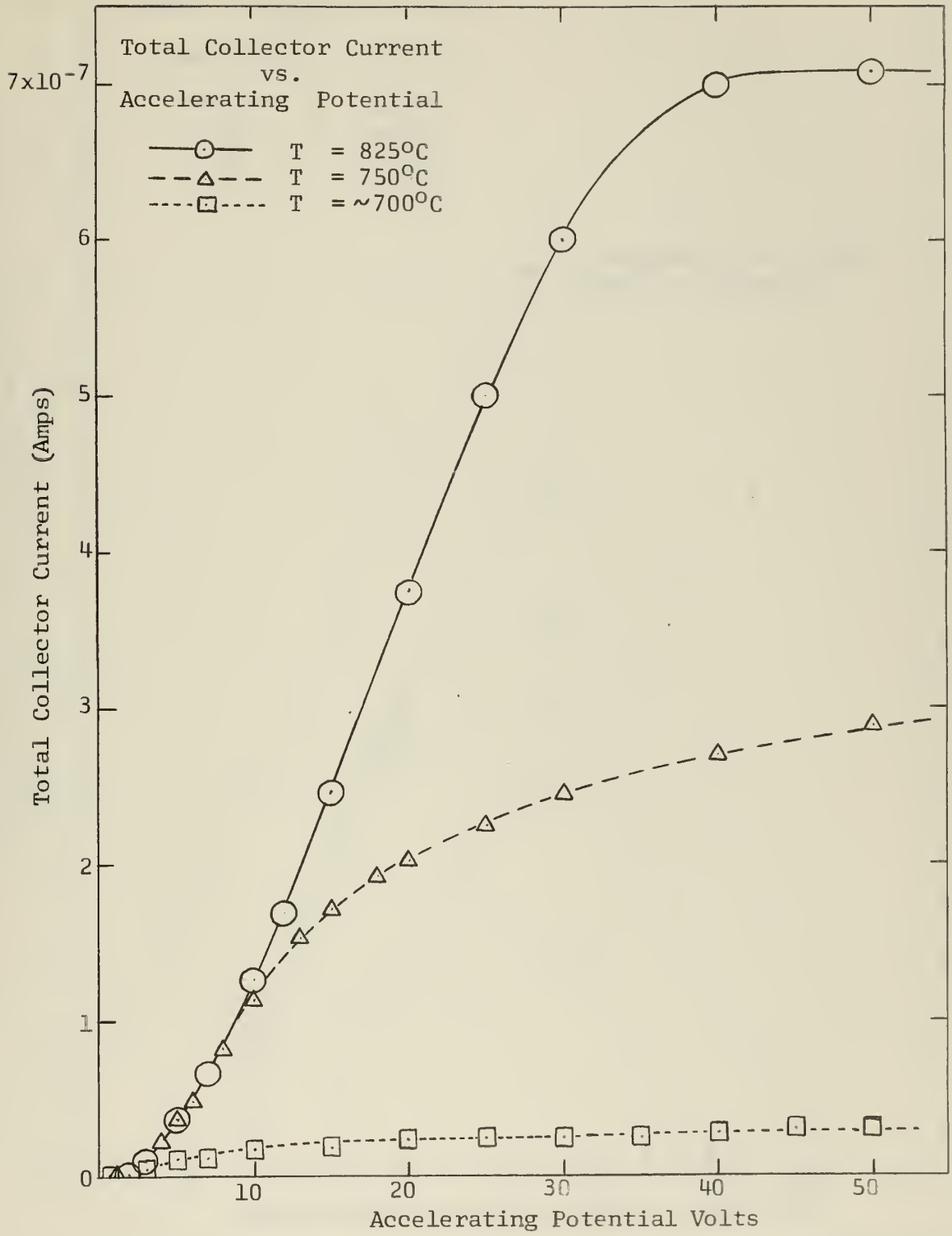

Figure 5. Total beam current as a function of accelerating potential.

Figure 6

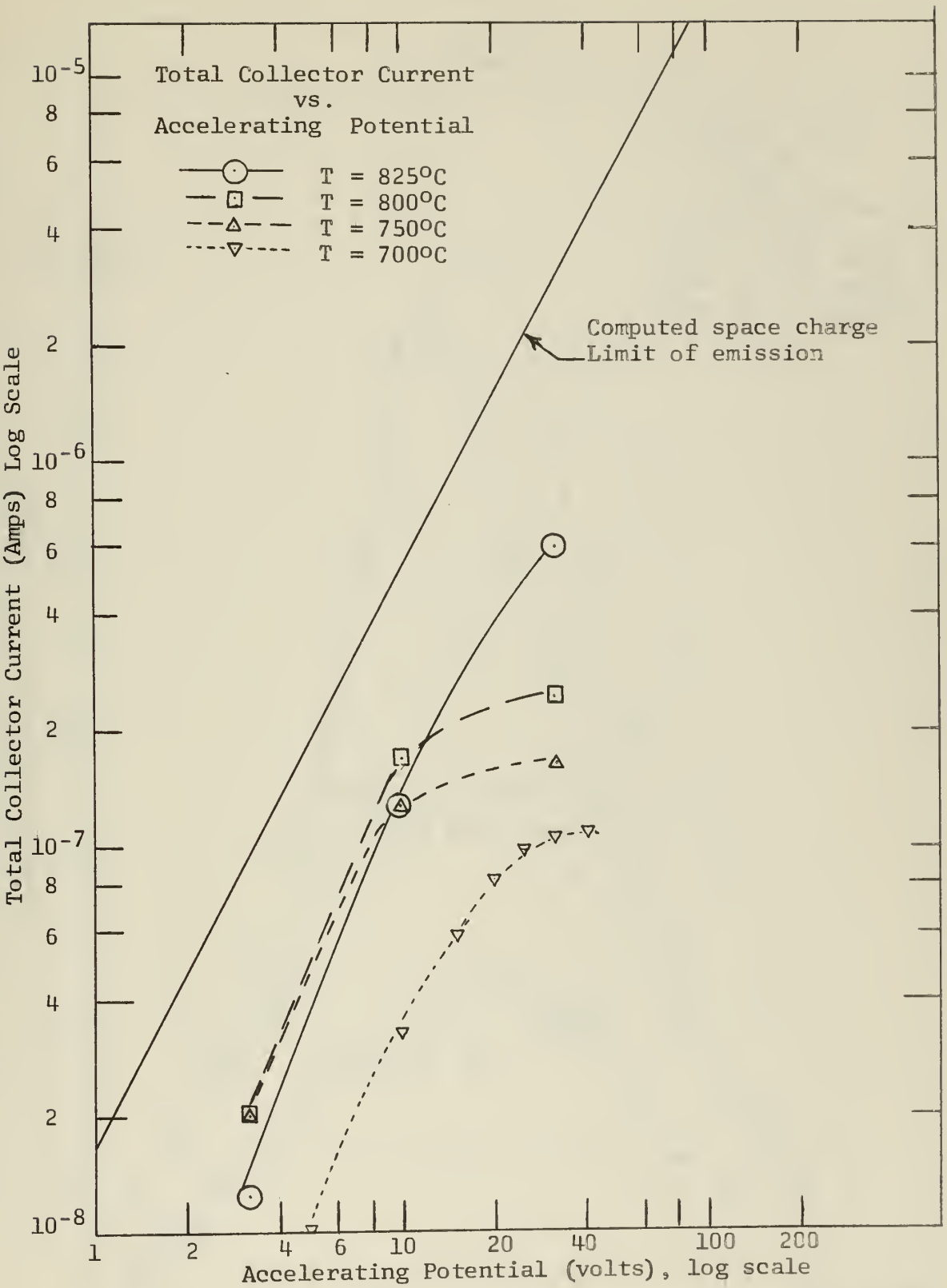

Figure 6. Total beam currents as a function of accelerating potential, comparison with space charge limited emission current.

Figure 7

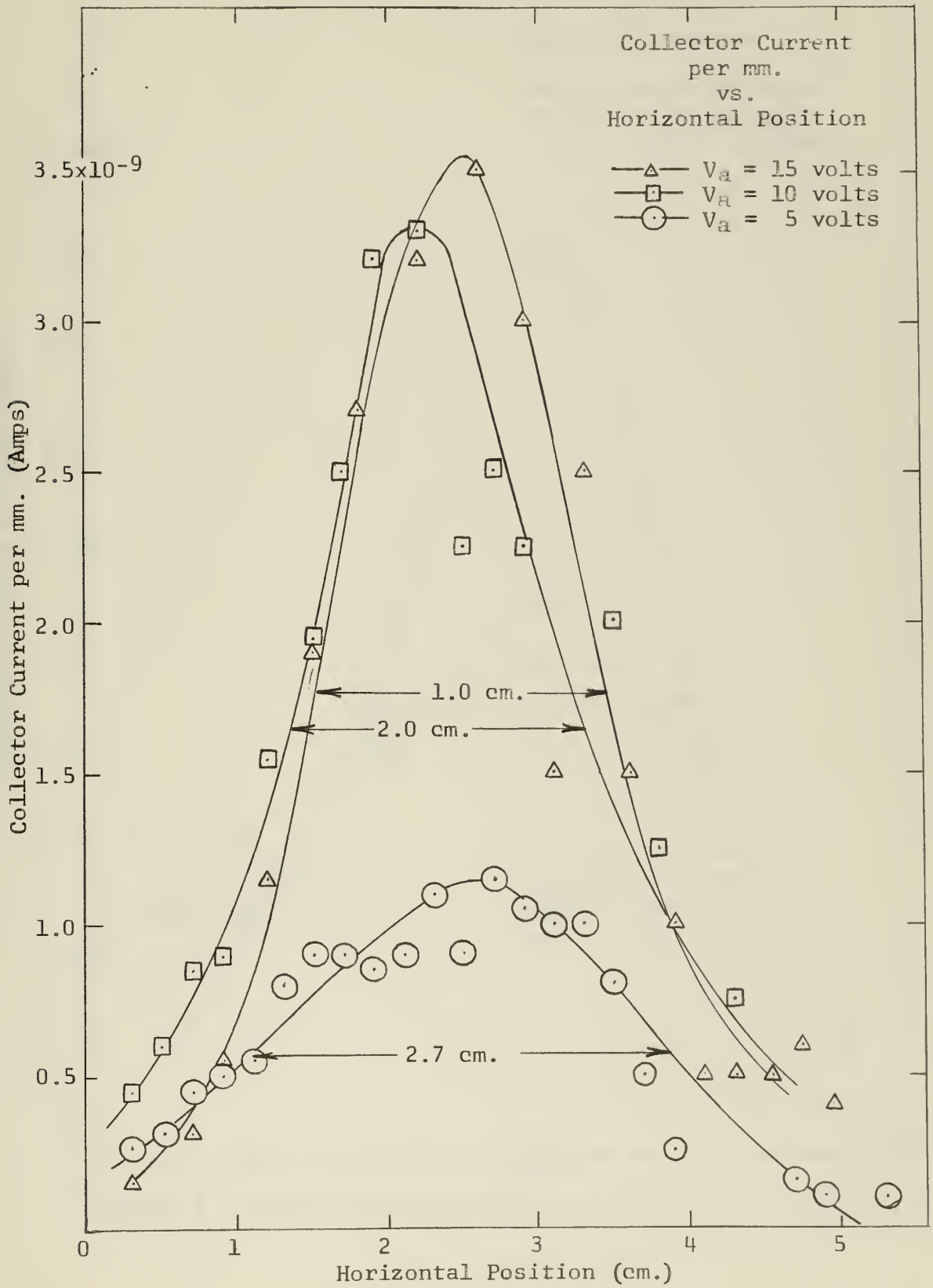

Figure 7. Horizontal Beam Profile at x = 6.7 cm.

Figure 8

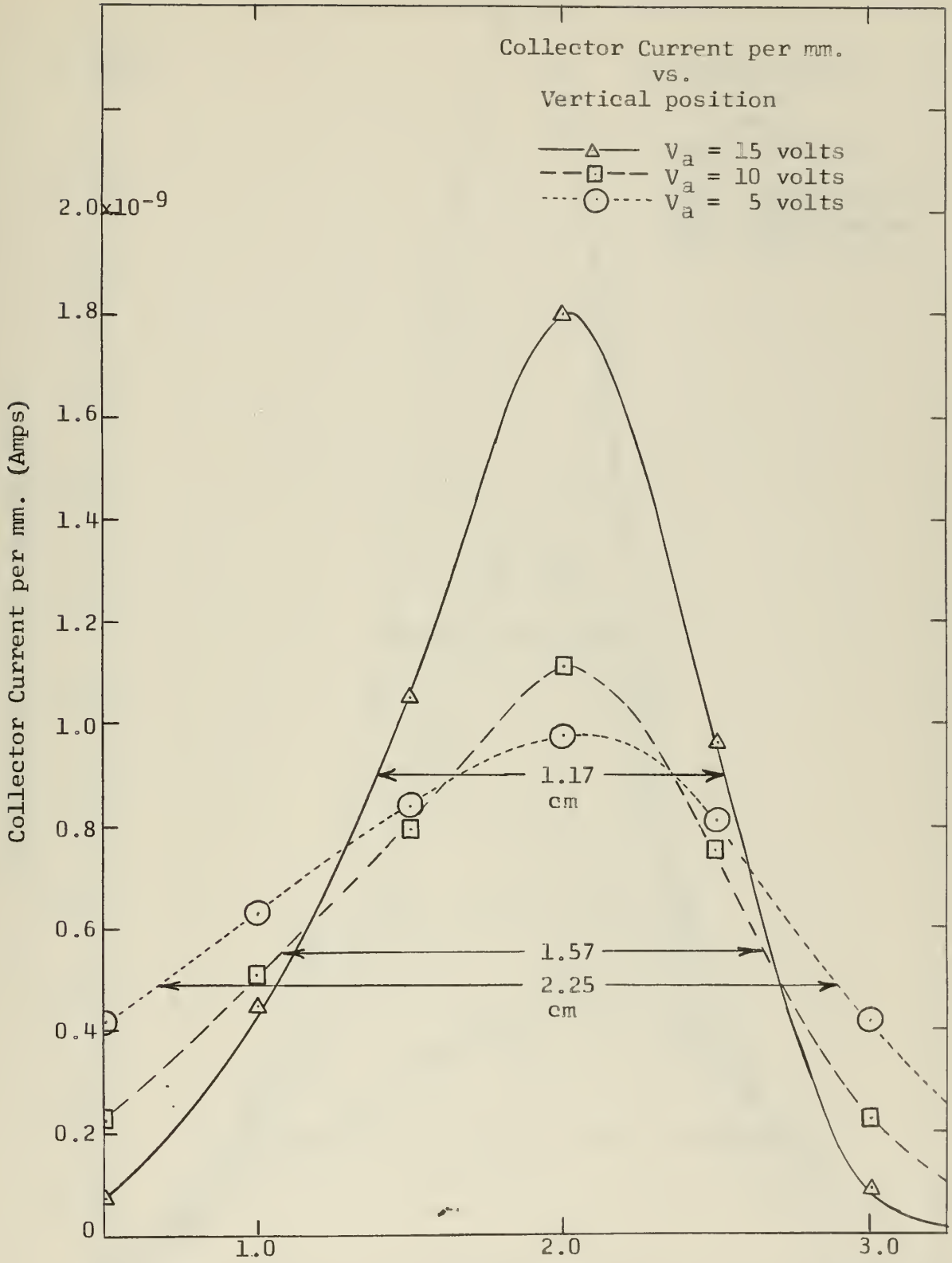

Figure 8. Vertical beam profile; x = 6.7 cm., T = 825^{o}C.

Figure 9

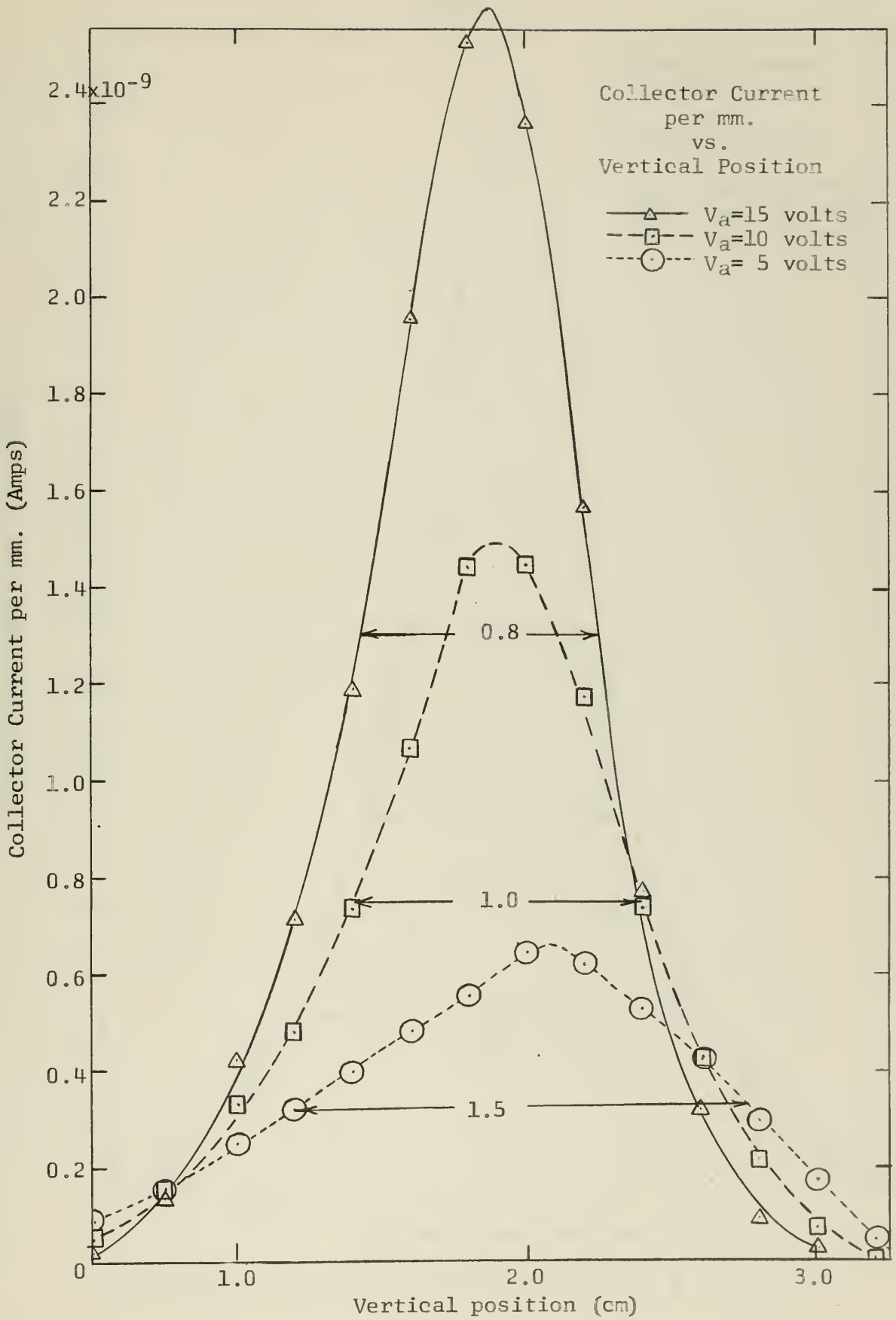

Figure 9. Vertical Profile, x = 5.1 cm, T = 825°C

Figure 10

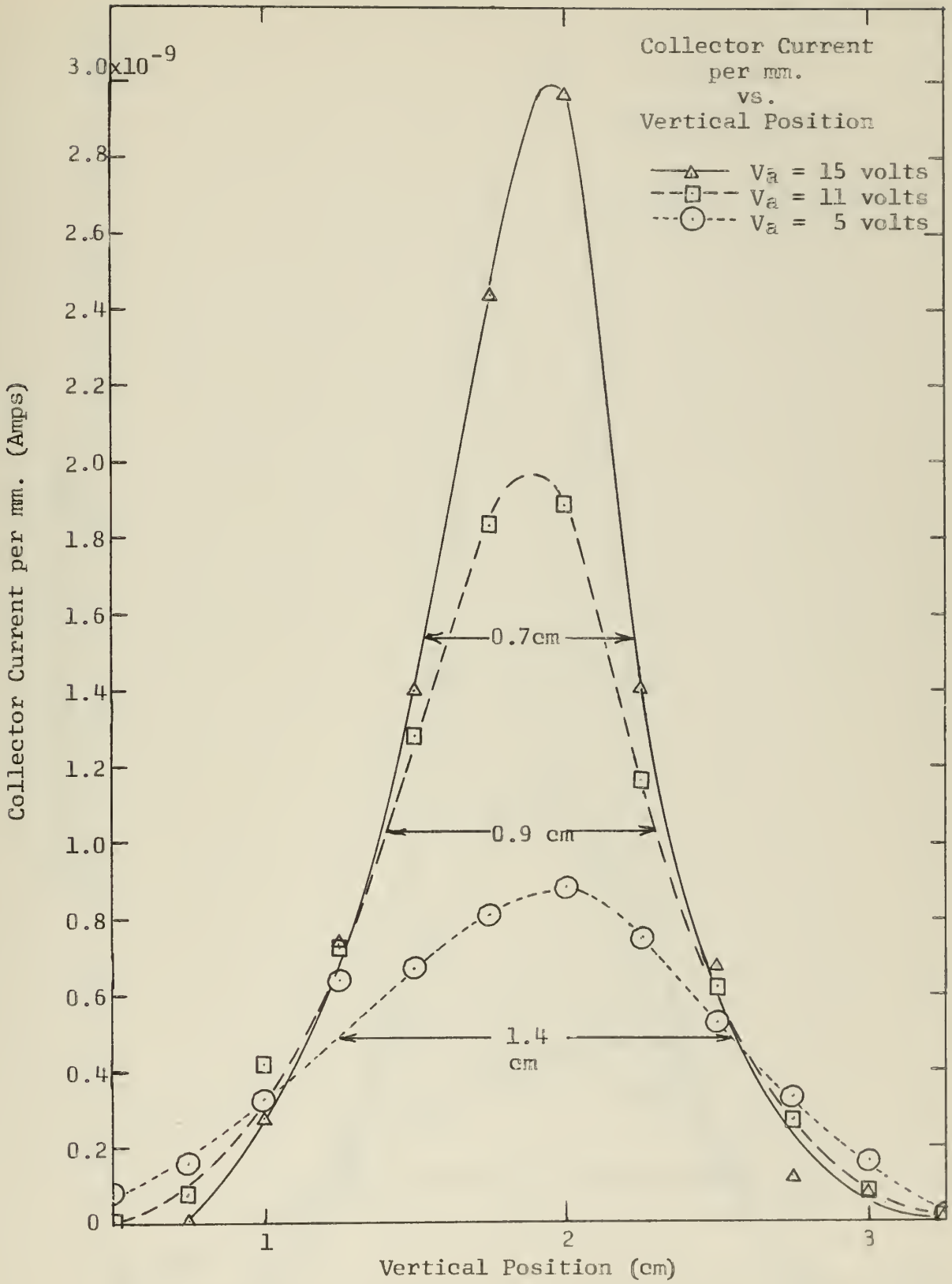

Fig7re 10. Vertical Profile; x = 3.2 cm, T = 825°C

Figure 11

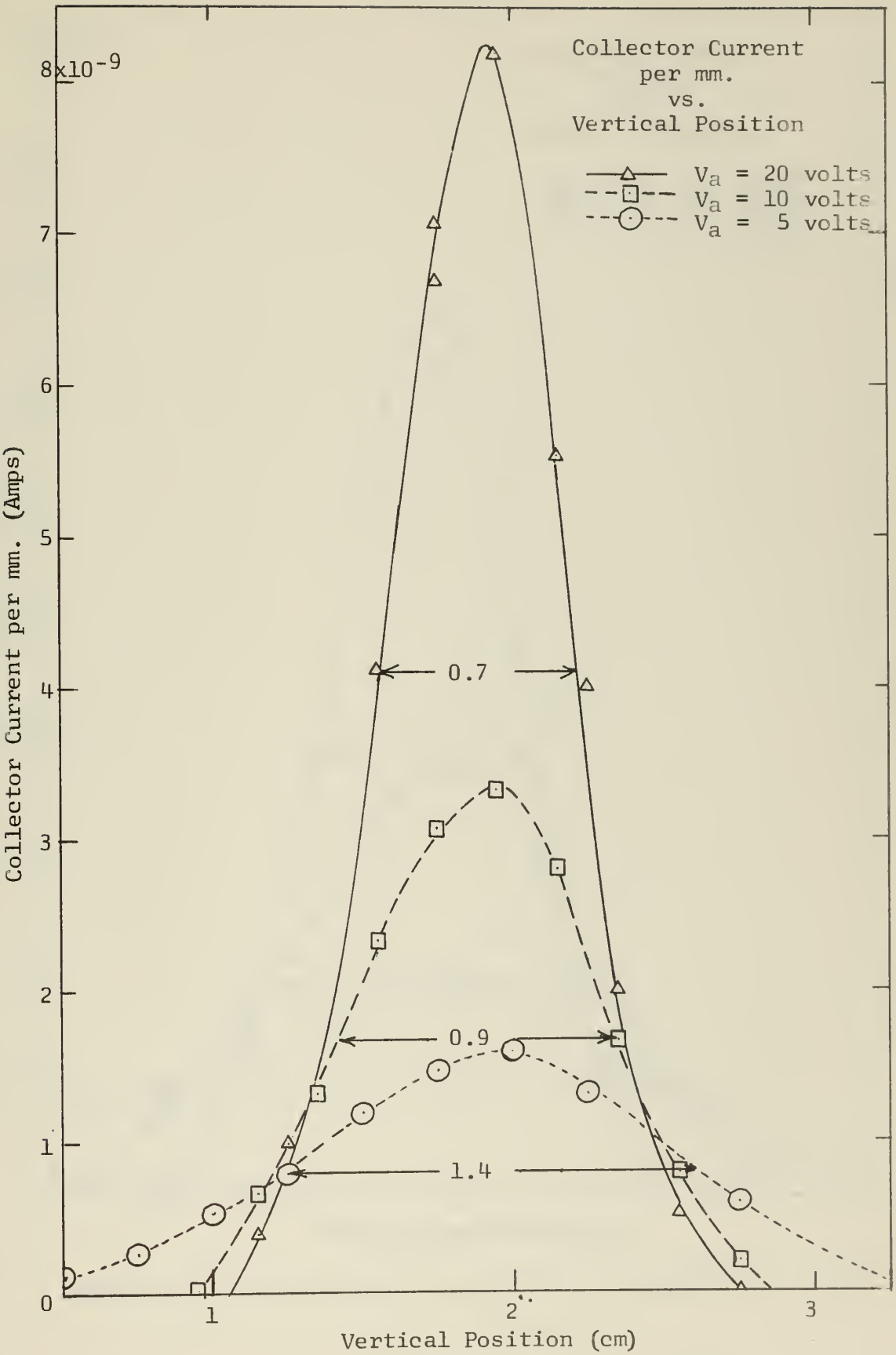

Figure 11. Vertical Profile; x = 3.2 cm, T = 825°C

Figure 12

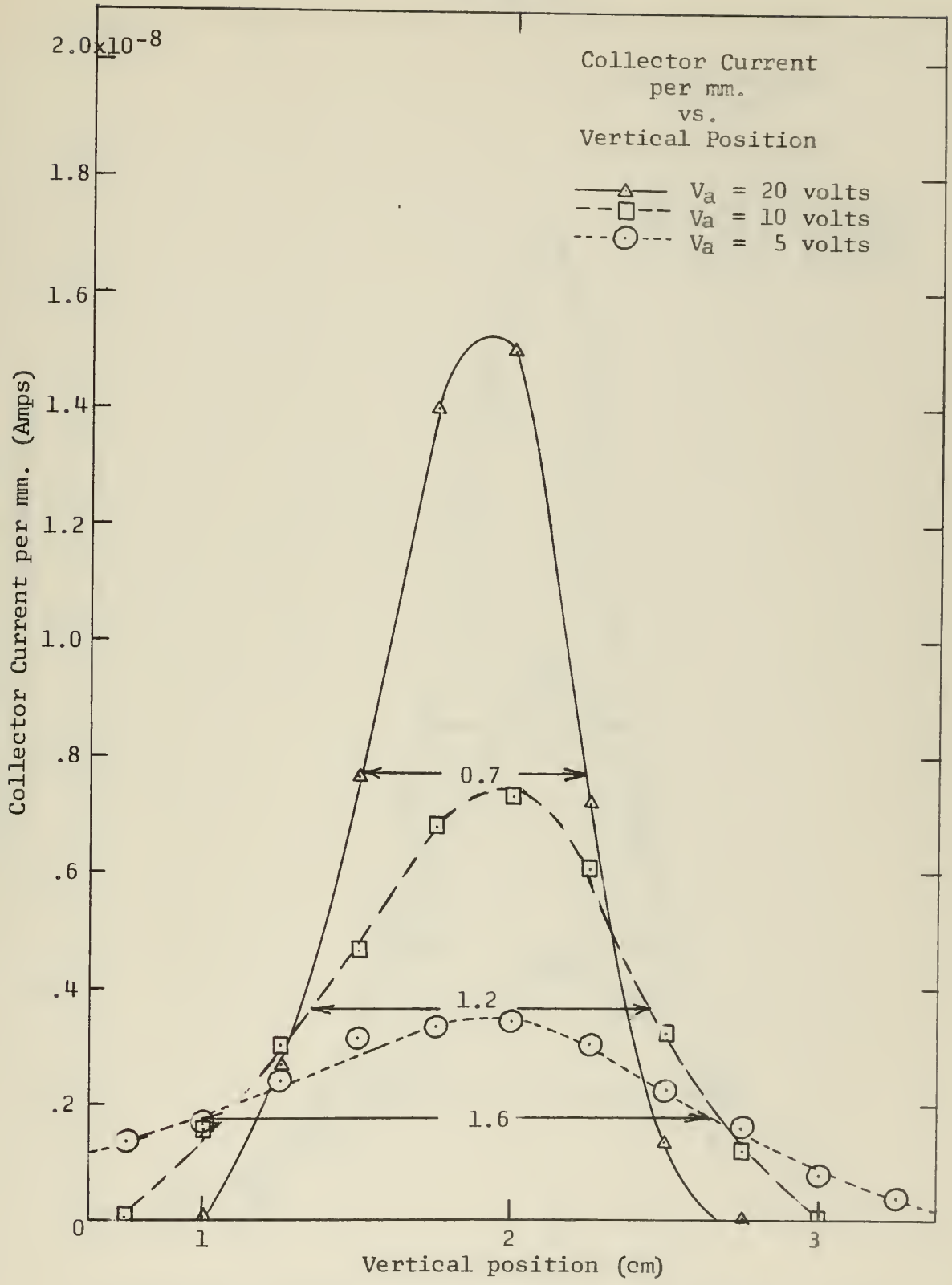

Figure 12. Vertical Profile; x = 3.2, T = 870°C

Figure 13

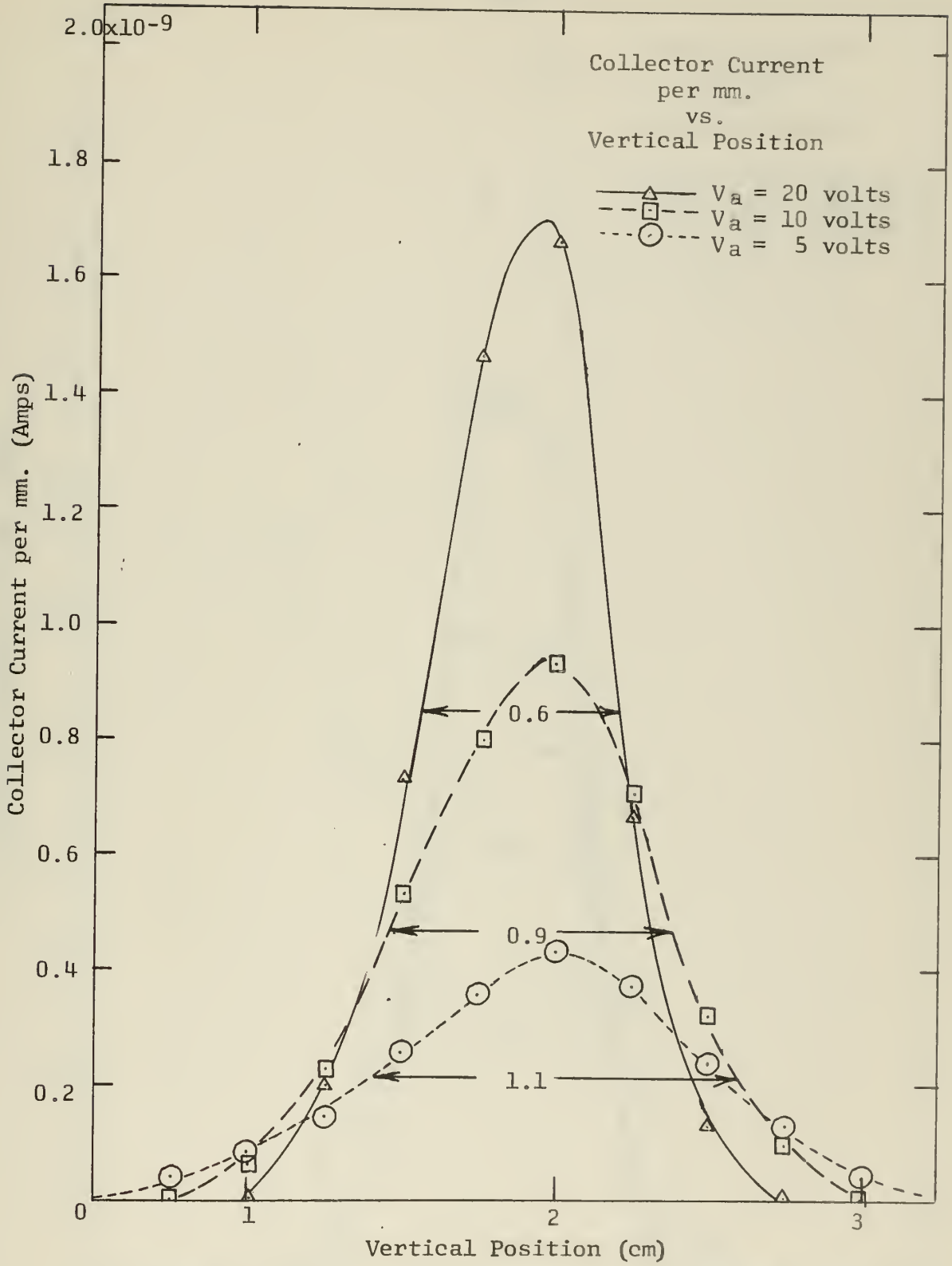

Figure 13. Vertical beam Profile; x = 3.2 cm, T - 790^{0}C

Figure 14

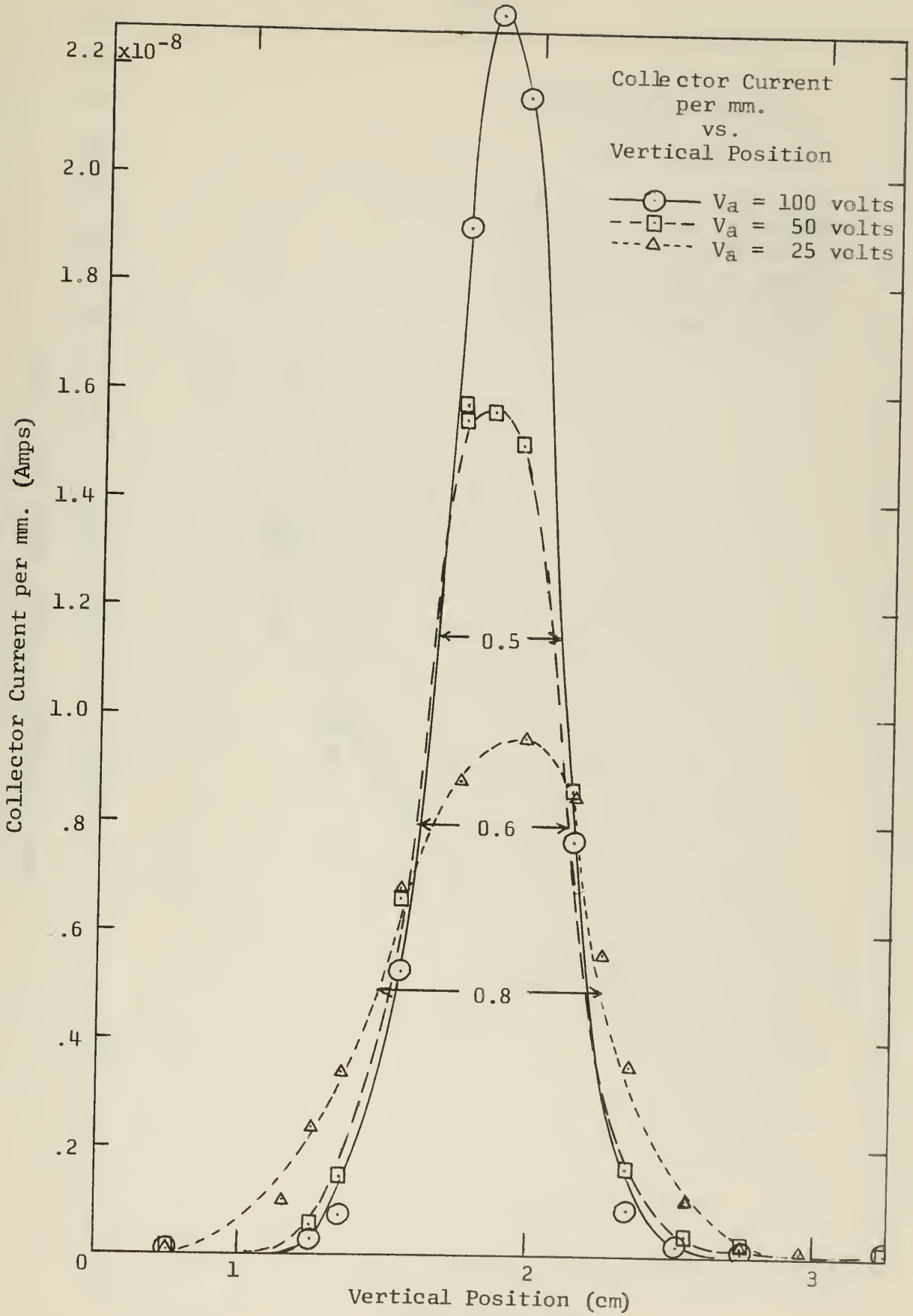

Figure 14. Vertical Profiles at Higher energies; x = 5.0 cm, T = 810°C

Figure 15

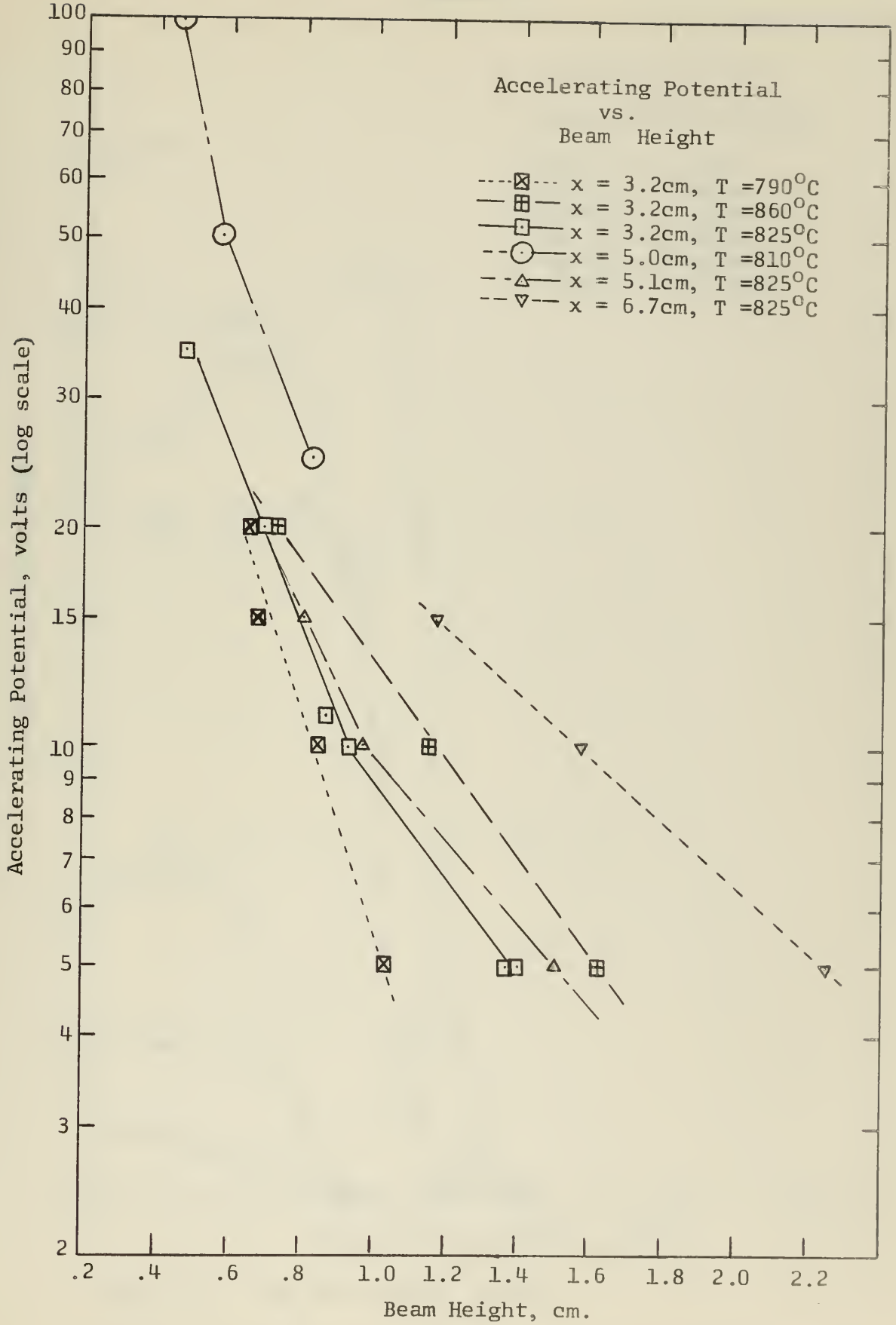

Figure 15. Beam Heights as a function of the accelerating Potential

Figure 16

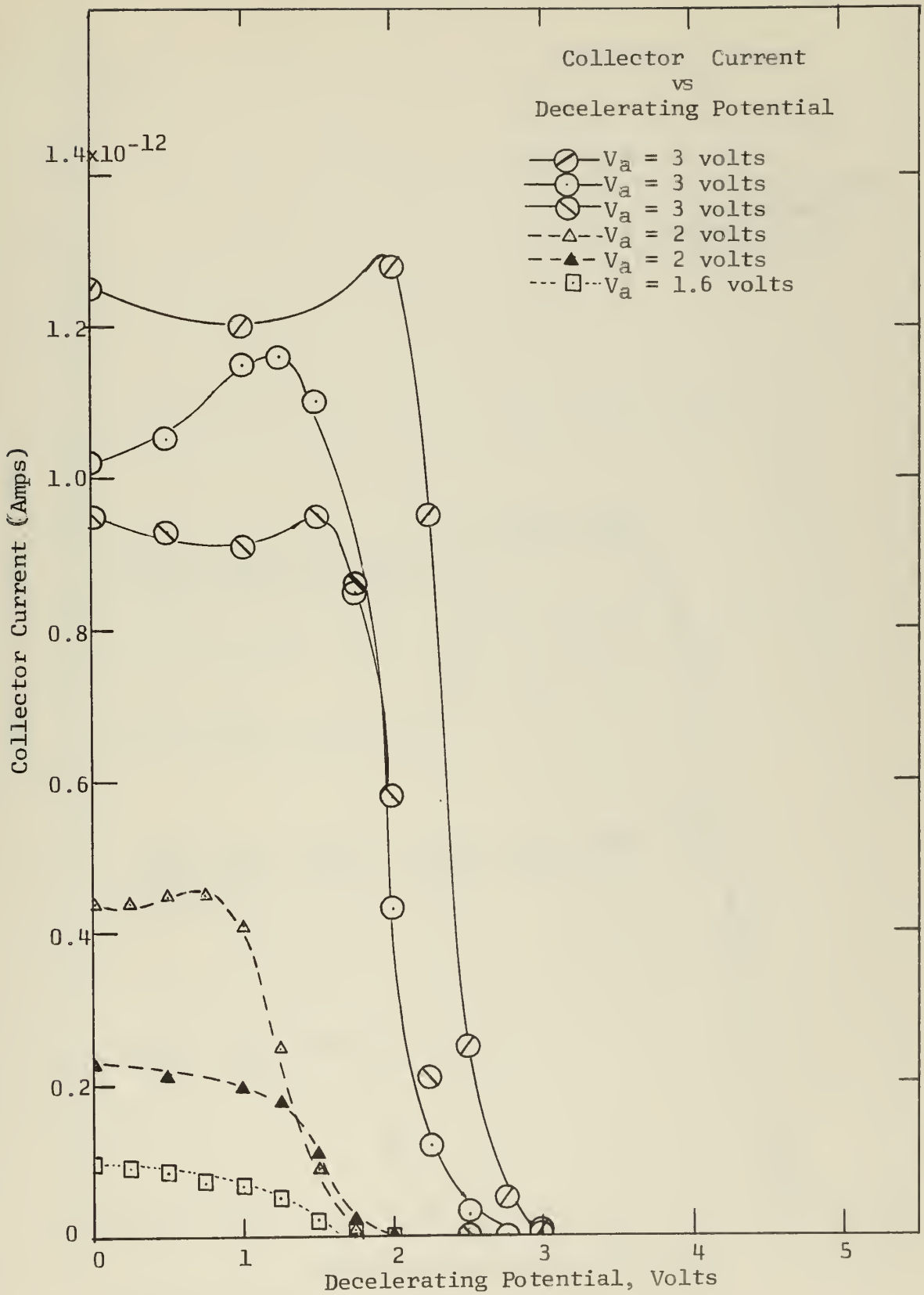

Figure 16. Ion Beam Energy Curves

Figure 17

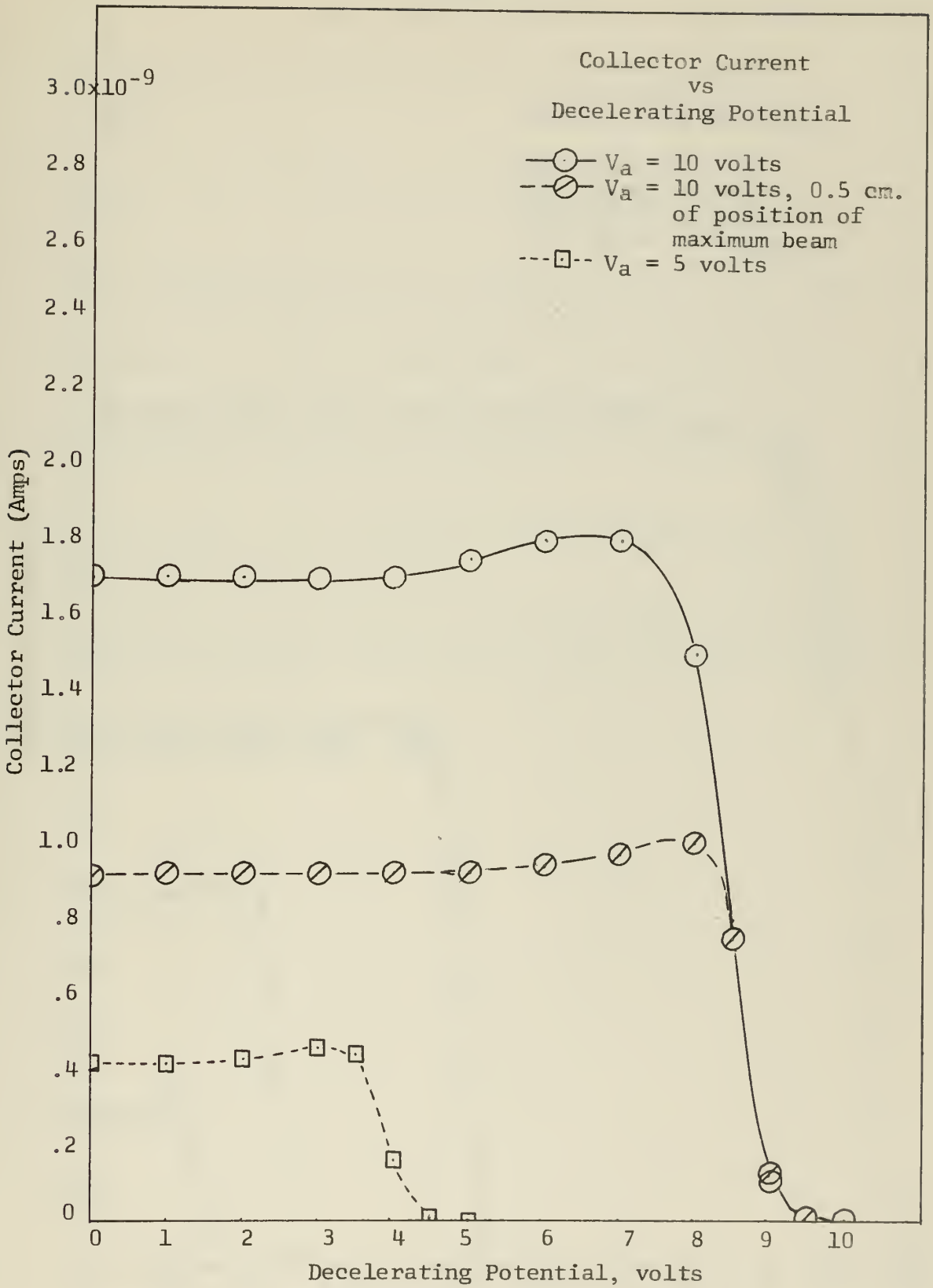

Figure 17. Ion beam energy curves

Figure 18

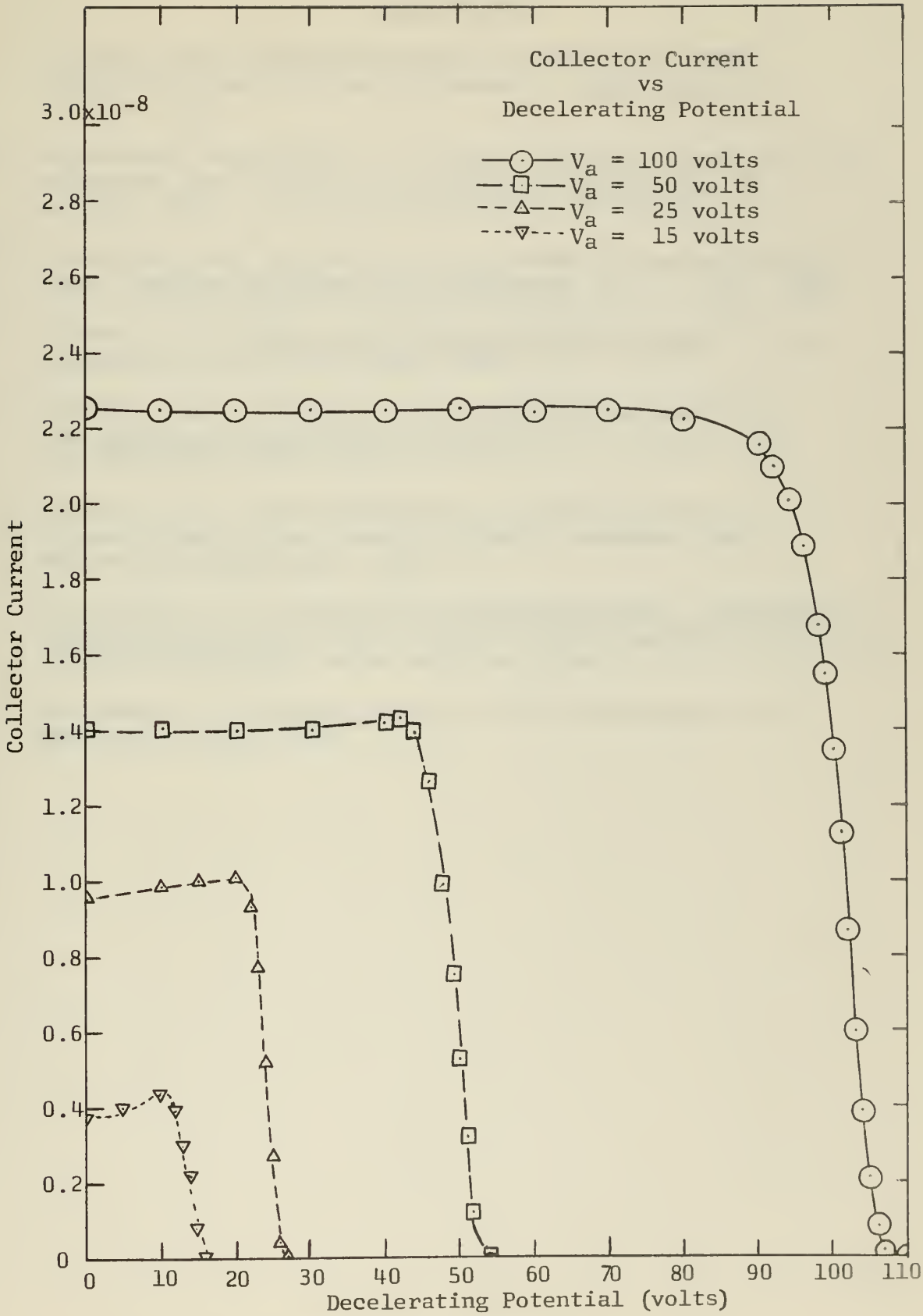

Figure 18. Ion Beam energy curves

BIBLIOGRAPHY

1. Skinner, G.T.; "Molecular Beams for the Study of High-Temperature-Gas Collision Processes", Phys. Fluids, 4, p. 1172, 1961

2. Kantrowitz, A. and Grey, J.; "A High Intensity Source for the Molecular Beam"; Review of Scientific Instruments, 22, p. 328, 1951.

3. Utterback, N.G. and Millter, G.H., "Fast Molecular Nitrogen Beam"; Review of Scientific Instruments, 32, p. 1101, 1961.

4. Pierce, J.R.; Theory and Design of Electron Beams; D. van Nostrand Co., Inc., New York, 1954.

5. Allison, S.K., and Kamegai, M.; "Lithium Ion Sources"; The Review of Scientific Instruments; Vol. 32, No. 10; pp. 1090-1092, Oct. 1961.

6. Waldron, J.C.; "The Preparation of Beta-Eucryptite"; United Kingdom Atomic Energy Authority Research Group Memorandum (AERE-M952); 1962.

7. Von Ardenne. M.; Tabellen der Elektronenphysik, Ionenphysik Und Ubermikroskopie, Band I; pp. 507-519; Hauptgebiete, Berlin; Deutscher Verlag der Wissenschafter, 1956.

8. Klemperer, O.; Electron Optics; p. 269; Cambridge at the Unitersity Press, 1953.

APPENDIX 1.

Description of Vacuum System and the Experimental Chamber

The Vacuum System

The vacuum system is a CHA Industries S-600 series high vacuum pumping system. The major components of this system are a 15 cubic feet per minute mechanical roughing pump (Welsh Duo Seal), a six inch purifying diffusion pump (NRC HS6-1500), a water cooled chevron type baffle, and a two liter stainless steel liquid nitrogen cold trap. Figure 19 is a schematic of the vacuum system in which the major components are shown. The vacuum system is controlled by five manually operated valves as shown in Fig. 1. Within the vacuum system are located two Hastings Thermocouple pressure gauges and one Bayard Alpert type Ion guage. One thermocouple gauge is located between the diffusion pump and the foreline valve and indicates the pressure into which the diffusion pump is discharging. The other Thermocouple gauge is located in the back fill line and indicates the pressure in the experimental chamber. The ion gauge is located in the body of the high vacuum valve adjacent to the liquid nitrogen trap. This gauge indicates the pressure on the diffusion pump side of the high vacuum valve when the high vacuum valve is closed. When the high vacuum valve is open the pressure indicated by this gauge is related to the pressure in the experimental chamber. There is also an ion gauge located in the experimental chamber for accurate indications of the working pressure. All pressure gauges are controlled by an F.J. Cooke, Inc. model #IGC-60-12

Figure 19

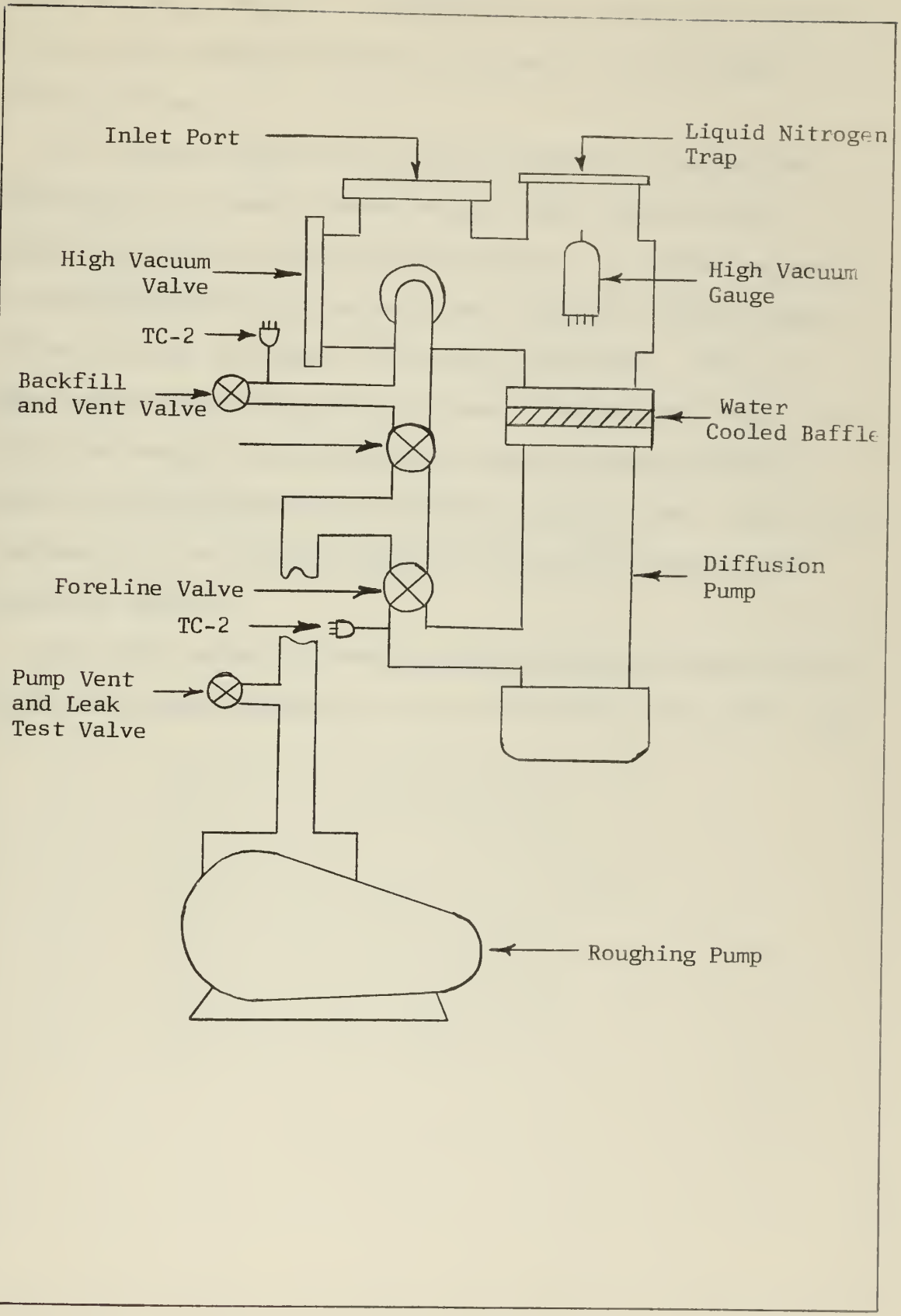

Figure 19. Schematic High Vacuum System

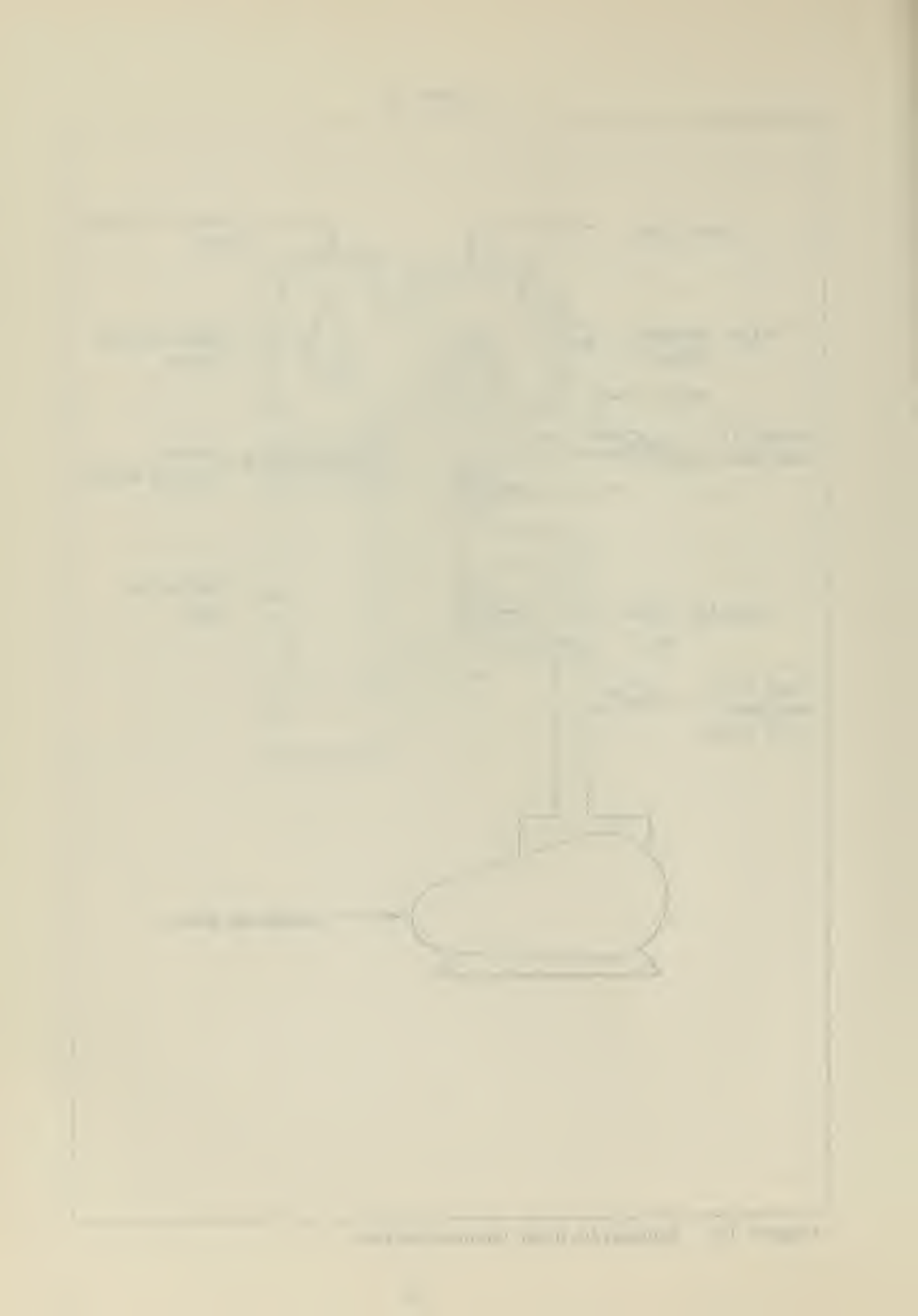

Ionization gauge control. The range of the thermocouple gauges is one to 1000 microns of Hg and the range of the ion gauges is 10^{-3} to 10^{-9} torr.

The diffusion pump of the vacuum system is protected from overheating by a Fenwall thermo-switch which is physically attached to the wall of the diffusion pump. The diffusion pump is also protected by a relay which will turn the diffusion pump off any time the ion gauge in use turns itself off. The ion gauge automatically turns off any time it exceeds full scale. A protection curcuit by-pass switch has been provided to allow operation without having an Ion gauge on at all times. Fig. 20 is a schematic of the wiring diagram of the vacuum system and its protection devices.

The normal operating pressure maintained by the vacuum system in the experimental chamber is 2.0×10^{-7} torr to 1.0×10^{-6} torr.

Figure 20

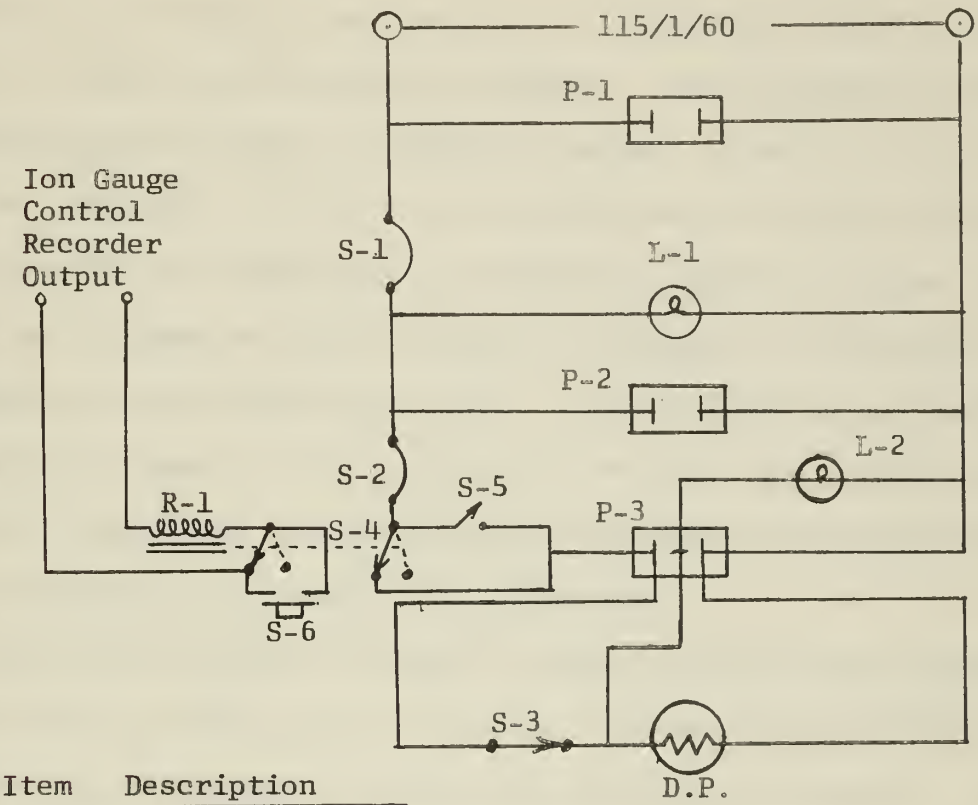

Item	Description
P-1	Vacuum Gauge Power Receptacle
S-1	Mechanical Pump Breaker Switch 30 Amp
L-1	Mechanical Pump Indicator Light
P-2	Mechanical Pump Power Receptacle
D.P.	Diffusion Pump
S-2	Diffusion Pump Breaker Switch 20 Amp
P-3	Diffusion Pump Receptacle
L-2	Diffusion Pump Indicator Light
S-3	Diffusion Pump Thermoswitch
S-4	Diffusion Pump Protection Relay
S-5	Protection Circuit Bypass
S-6	Protection Circuit Reset Switch
R-1	Protection Circuit Relay

Figure 20. Vacuum System Wiring Diagram

The Experimental Chamber

The experimental chamber of this system was designed and built to be as versatile as possible. The chamber consists of two parts, a "Tee" and a cylindrical chamber. The experimental chamber was constructed entirely of 6061-T6 aluminum. Schedule 40 six inch pipe was used for the "Tee" and all parts except the three inch port in the top of the "Tee" which is schedule 5, three inch pipe. The "Tee" has a flange at each end which is designed to accomodate a standard six inch high vacuum valve. It is planned to add another cylindrical chamber to the other end of the "Tee" at a later date to give a capability of operating either chamber at any given time or of operating both chambers simultaneously.

The main cylindrical chamber is made from 3/16 inch aluminum sheet which is formed into a cylinder. The inside dimensions of the cylinder are ten inches in height and 18 inches in diameter. One inch aluminum is used for the base and for the flange. All welds are heliarc, vacuum tight welds located on the inside of the chamber where possible. The cylindrical chamber has three six inch access ports and a removable top for easy access to the experiment. The rear flange has twelve electrical feed-throughs in two concentric circles. The front flange has eight electrical feed-throughs and two and one-half inch lucite window. The other flange can accomodate a Wilson-type vacuum seal through which a horizontal probe may be mounted. The top flange is removable by means of a rope hoist. A Wilson-type vacuum seal is located in the center of

the top flange. This seal accomodates a 1/4 inch rod upon which is mounted the ion collector. The collector may be moved vertically to obtain the beam profile. Figure 21 is a sketch of the experimental chamber and vacuum "Tee". The ion gun is shown as it is mounted in the experimental chamber.

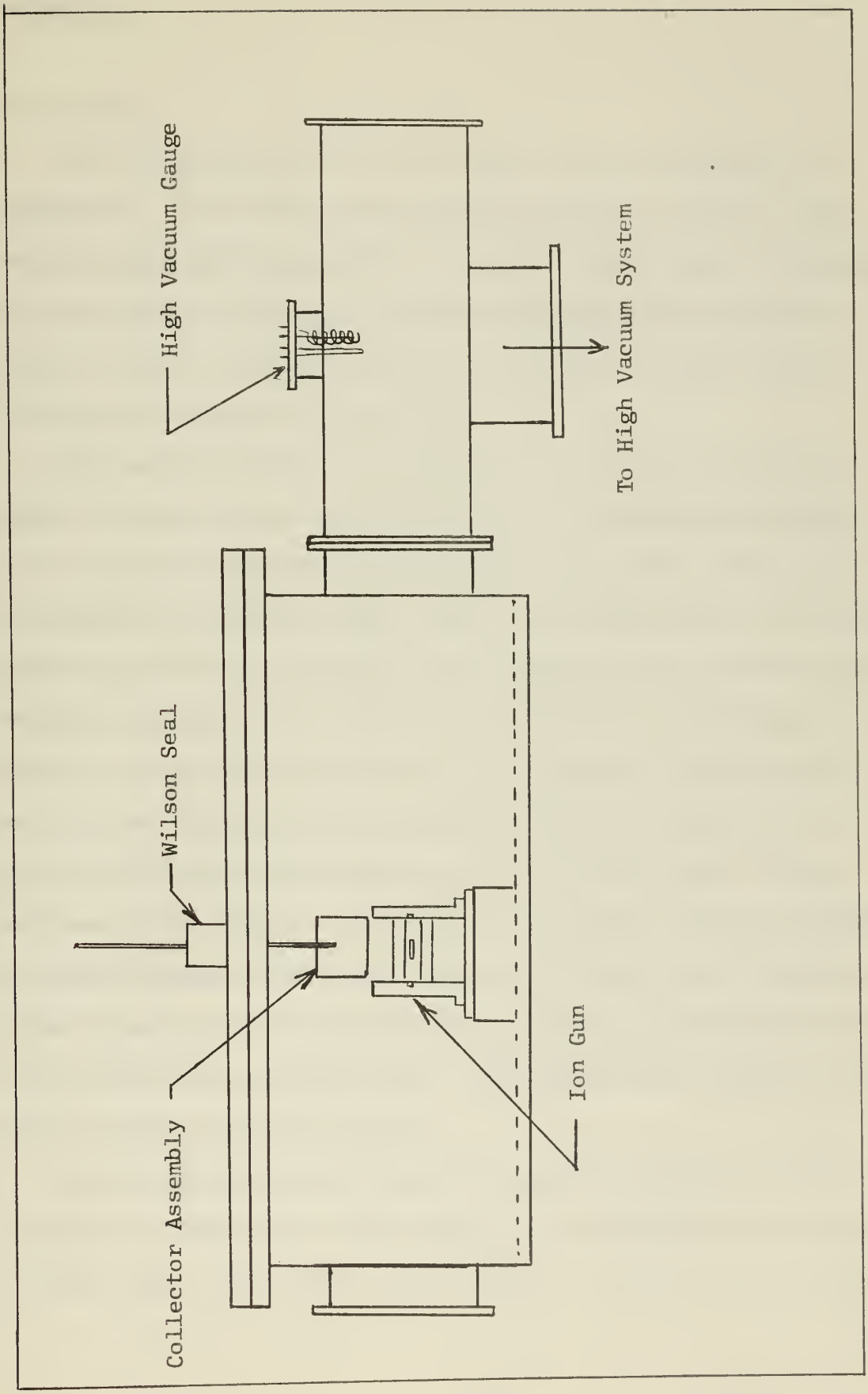

Figure 21. Experimental Chamber and Vacuum "Tee" showing the position of the ion gun as mounted in the chamber

Appendix 2.

The Ion Gun

The ion gun consists of an emitter and two accelerating electrodes. The emitter boat and electrodes are made of 0.005 inch tantalum and are mounted in a lavite holder that is designed for the maximum freedom in varying parameters such as position within the gun, and inter electrode distance. Figure 1 shows the salient features of the ion gun.

The emitter surface is the face of a 1.0 by 1.5 cm. boat which is three to four millimeters deep. The emitter is heated by a 0.010 inch tungsten filament which is wound in a flat coil and embedded in alumdum cement inside the emitter boat. The area behind the emitter is protected from radiation by a pair of nickel radiation shields and a stainless steel holder. The filament is heated by a variable zero to 24 volt DC supply. Both AC and DC sources have been used for heating the filament, however it is now believed that the DC heater source has less effect on the portions of the circuit. Initially a 0.005 inch tungsten filament was used, however it was found that this filament gave too much concentrated heat at the point where the heater filament was joined to the 0.020 inch platinum leads. These leads are joined to the heater filament by spot welding.

Several methods were tried for securely adhering the beta-eucryptite to the face of the emitter. The powdered beta-eucryptite is mixed into a slurry with amyl acetate. A small trace of Parlodion,

a form of non-explosive cellulose nitrate, may be added to the slurry as a plasticizer. This increases the bonding together of the coating but it is not believed to increase the bonding to the face of the tantalum boat. The addition of the Parlodium tends to increase the porosity of the beta-eucryptite. The surface of the beta-eucryptite appeared powdery and rough when the Parlodium was used but appeared smooth when the Parlodium was not used. The slurry of beta-eucryptite was first painted directly on the smooth face of the tantalum boat. Three coats were used and each dried with a heat lamp to evaporate the amyl acetate. This method worked well but the beta-eucryptite tended to flake off in large chunks if an attempt was made to move or adjust the emitter. In an effort to avoid this flaking action, the face of the tantalum boat was scored in a criss-cross pattern to a depth of approximately 0.005 inch. There was not as much flaking off in this configuration as in the first but the flaking was still appreciable when Parlodium was added to the slurry. The third method used was to weld a very fine tungsten mesh over the face of the tantalum boat. This method worked very satisfactorily in that there was no flaking off of the beta-eucryptite. However, the entire mass of beta-eucryptite and tungsten mesh would lose physical contact with the face of the tantalum boat during heating. The beta-eucryptite is an extremely poor conductor of heat or electricity. When the emitting substance lost physical contact with the tantalum boat it took a higher tantalum temperature to achieve the working temperature on the face of the beta-eucryptite. The tungsten mesh did minimize the problem of a potential drop between the tantalum boat and the face of the

beta-eucryptite because the embedded mesh was at the same potential as the tantalum boat and rear accelerating electrode. The initial heating of the beta-eucryptite was done very slowly. The temperature was gradually raised until an increase in pressure was noted on the ion gauge, the temperature was held at this point until the pressure began to fall. This procedure was followed until operating temperature was reached.

The accelerating electrodes are formed into a Pierce geometry to obtain maximum beam density under space charge limiting conditions. This design produces a slightly convergent beam which will become divergent further down the stream. The rear electrode has a one centimeter by one and one-half centimeter opening to accomodate the thermionic emitter. The opening in the front electrode is one cm. by 0.47 cm. Normal separation between electrodes is one centimeter. The rear electrode is maintained at a positive potential equal to the desired energy of the beam. The electrodes are mounted on Lavite formers which are adjustable in a track in the main body of the gun. During the initial phase of the experiment, 0.001 inch tantalum foil was used in the construction of the accelerating electrodes. The tantalum electrodes themselves give strength to the mount as a whole and it was found that the 0.001 inch tantalum foil was too thin for proper support and was easily distorted. Tantalum foil of 0.005 inch was adopted for use in the later stages of the experiment. This was found to be very satisfactory as far as strength was concerned but it was

more difficult to form to the precise geometry required. It has been proposed that 0.003 inch tantalum foil be used for the next modification.

The accelerating potential is applied to the rear electrode and the emitter. The front electrode is at ground potential. This arrangement gives a grounded beam. Had we applied the accelerating potential to the front electrode then we would have had a "hot" beam and would have had to detect the beam with a collector at an equal potential to the accelerating potential.